Ca^{2+} entry mediate increased pulmonary and systemic vascular resistance in L-NAME-treated rats. *Am J Physiol Lung Cell Mol Physiol* 293: L1306–L1313, 2007.

22. **Do e Z, Fukumoto Y, Takaki A, Tawara S, Ohashi J, Nakano M, Tada T, Saji K, Sugimura K, Fujita H, Hoshikawa Y, Nawata J, Kondo T, Shimokawa H.** Evidence for Rho-kinase activation in patients with pulmonary arterial hypertension. *Circ J* 73: 1731–1739, 2009.
23. **Etienne-Manneville S, Hall A.** Rho GTPases in cell biology. *Nature* 420: 629–635, 2002.
24. **Eto Y, Shimokawa H, Hiroki J, Morishige K, Kandabashi T, Matsumoto Y, Amano M, Hoshijima M, Kaibuchi K, Takeshita A.** Gene transfer of dominant negative Rho kinase suppresses neointimal formation after balloon injury in pigs. *Am J Physiol Heart Circ Physiol* 278: H1744–H1750, 2000.
25. **Fukata Y, Amano M, Kaibuchi K.** Rho-Rho-kinase pathway in smooth muscle contraction and cytoskeletal reorganization of non-muscle cells. *Trends Pharmacol Sci* 22: 32–39, 2001.
26. **Fukui S, Fukumoto Y, Suzuki J, Saji K, Nawata J, Tawara S, Shinozaki T, Kagaya Y, Shimokawa H.** Long-term inhibition of Rho-kinase ameliorates diastolic heart failure in hypertensive rats. *J Cardiovasc Pharmacol* 51: 317–326, 2008.
27. **Fukumoto Y, Matoba T, Ito A, Tanaka H, Kishi T, Hayashidani S, Abe K, Takeshita A, Shimokawa H.** Acute vasodilator effects of a Rho-kinase inhibitor, fasudil, in patients with severe pulmonary hypertension. *Heart* 91: 391–392, 2005.
28. **Funakoshi Y, Ichiki T, Shimokawa H, Egashira K, Takeda K, Kaibuchi K, Takeya M, Yoshimura T, Takeshita A.** Rho-kinase mediates angiotensin II-induced monocyte chemoattractant protein-1 expression in rat vascular smooth muscle cells. *Hypertension* 38: 100–104, 2001.
29. **Gavazzi G, Deffert C, Trocme C, Schappi M, Herrmann FR, Krause KH.** NOX1 deficiency protects from aortic dissection in response to angiotensin II. *Hypertension* 50: 189–196, 2007.
30. **Griendling KK, Berk BC, Ganz P, Gimbrone MA Jr, Alexander RW.** Angiotensin II stimulation of vascular smooth muscle phosphoinositide metabolism. State of the art lecture. *Hypertension* 9: III181–III185, 1987.
31. **Griendling KK, FitzGerald GA.** Oxidative stress and cardiovascular injury: Part II: animal and human studies. *Circulation* 108: 2034–2040, 2003.
32. **Griendling KK, Minieri CA, Ollerenshaw JD, Alexander RW.** Angiotensin II stimulates NADH and NADPH oxidase activity in cultured vascular smooth muscle cells. *Circ Res* 74: 1141–1148, 1994.
33. **Guilluy C, Bregeon J, Toumaniantz G, Rolli-Derkinderen M, Retailleau K, Loufrani L, Henrion D, Scalbert E, Bril A, Torres RM, Offermanns S, Pacaud P, Loirand G.** The Rho exchange factor Arhgef1 mediates the effects of angiotensin II on vascular tone and blood pressure. *Nat Med* 16: 183–190, 2010.
34. **Hall A.** Rho GTPases and the actin cytoskeleton. *Science* 279: 509–514, 1998.
35. **Hattori T, Shimokawa H, Higashi M, Hiroki J, Mukai Y, Kaibuchi K, Takeshita A.** Long-term treatment with a specific Rho-kinase inhibitor suppresses cardiac allograft vasculopathy in mice. *Circ Res* 94: 46–52, 2004.
36. **Hattori T, Shimokawa H, Higashi M, Hiroki J, Mukai Y, Tsutsui H, Kaibuchi K, Takeshita A.** Long-term inhibition of Rho-kinase suppresses left ventricular remodeling after myocardial infarction in mice. *Circulation* 109: 2234–2239, 2004.
37. **Higashi M, Shimokawa H, Hattori T, Hiroki J, Mukai Y, Morikawa K, Ichiki T, Takahashi S, Takeshita A.** Long-term inhibition of Rho-kinase suppresses angiotensin II-induced cardiovascular hypertrophy in rats in vivo: effect on endothelial NAD(P)H oxidase system. *Circ Res* 93: 767–775, 2003.
38. **Hiroki J, Shimokawa H, Higashi M, Morikawa K, Kandabashi T, Kawamura N, Kubota T, Ichiki T, Amano M, Kaibuchi K, Takeshita A.** Inflammatory stimuli upregulate Rho-kinase in human coronary vascular smooth muscle cells. *J Mol Cell Cardiol* 37: 537–546, 2004.
39. **Hizume T, Morikawa K, Takaki A, Abe K, Sunagawa K, Amano M, Kaibuchi K, Kubo C, Shimokawa H.** Sustained elevation of serum cortisol level causes sensitization of coronary vasoconstricting responses in pigs in vivo: a possible link between stress and coronary vasospasm. *Circ Res* 99: 767–775, 2006.
40. **Inoue T, Node K.** Molecular basis of restenosis and novel issues of drug-eluting stents. *Circ J* 73: 615–621, 2009.
41. **Ito K, Hirooka Y, Kishi T, Kimura Y, Kaibuchi K, Shimokawa H, Takeshita A.** Rho/Rho-kinase pathway in the brainstem contributes to hypertension caused by chronic nitric oxide synthase inhibition. *Hypertension* 43: 156–162, 2004.
42. **Ito K, Hirooka Y, Sakai K, Kishi T, Kaibuchi K, Shimokawa H, Takeshita A.** Rho/Rho-kinase pathway in brain stem contributes to blood pressure regulation via sympathetic nervous system: possible involvement in neural mechanisms of hypertension. *Circ Res* 92: 1337–1343, 2003.
43. **Itoh T, Nagaya N, Murakami S, Fujii T, Iwase T, Ishibashi-Ueda H, Yutani C, Yamagishi M, Kimura H, Kangawa K.** C-type natriuretic peptide ameliorates monocrotaline-induced pulmonary hypertension in rats. *Am J Respir Crit Care Med* 170: 1204–1211, 2004.
44. **Jin ZG, Lungu AO, Xie L, Wang M, Wong C, Berk BC.** Cyclophilin A is a proinflammatory cytokine that activates endothelial cells. *Arterioscler Thromb Vasc Biol* 24: 1186–1191, 2004.
45. **Jin ZG, Melaragno MG, Liao DF, Yan C, Haendeler J, Suh YA, Lambeth JD, Berk BC.** Cyclophilin A is a secreted growth factor induced by oxidative stress. *Circ Res* 87: 789–796, 2000.
46. **Kandabashi T, Shimokawa H, Miyata K, Kunihiro I, Eto Y, Morishige K, Matsumoto Y, Obara K, Nakayama K, Takahashi S, Takeshita A.** Evidence for protein kinase C-mediated activation of Rho-kinase in a porcine model of coronary artery spasm. *Arterioscler Thromb Vasc Biol* 23: 2209–2214, 2003.
47. **Kandabashi T, Shimokawa H, Miyata K, Kunihiro I, Kawano Y, Fukata Y, Higo T, Egashira K, Takahashi S, Kaibuchi K, Takeshita A.** Inhibition of myosin phosphatase by upregulated rho-kinase plays a key role for coronary artery spasm in a porcine model with interleukin-1beta. *Circulation* 101: 1319–1323, 2000.
48. **Kandabashi T, Shimokawa H, Mukai Y, Matoba T, Kunihiro I, Morikawa K, Ito M, Takahashi S, Kaibuchi K, Takeshita A.** Involvement of rho-kinase in agonists-induced contractions of arteriosclerotic human arteries. *Arterioscler Thromb Vasc Biol* 22: 243–248, 2002.
49. **Katsumata N, Shimokawa H, Seto M, Kozai T, Yamawaki T, Kuwata K, Egashira K, Ikegaki I, Asano T, Sasaki Y, Takeshita A.** Enhanced myosin light chain phosphorylations as a central mechanism for coronary artery spasm in a swine model with interleukin-1beta. *Circulation* 96: 4357–4363, 1997.
50. **Khromykh LM, Kulikova NL, Anfalova TV, Muranova TA, Abramov VM, Vasiliev AM, Khlebnikov VS, Kazansky DB.** Cyclophilin A produced by thymocytes regulates the migration of murine bone marrow cells. *Cell Immunol* 249: 46–53, 2007.
51. **Kikuchi Y, Yasuda S, Aizawa K, Tsuburaya R, Ito Y, Takeda M, Nakayama M, Ito K, Takahashi J, Shimokawa H.** Enhanced Rho-kinase activity in circulating neutrophils of patients with vasospastic angina—Possible biomarker for diagnosis and disease activity assessment. *J Am Coll Cardiol.* In press.
52. **Kim H, Kim WJ, Jeon ST, Koh EM, Cha HS, Ahn KS, Lee WH.** Cyclophilin A may contribute to the inflammatory processes in rheumatoid arthritis through induction of matrix degrading enzymes and inflammatory cytokines from macrophages. *Clin Immunol* 116: 217–224, 2005.
53. **Kimura K, Ito M, Amano M, Chihara K, Fukata Y, Nakafuku M, Yamamori B, Feng J, Nakano T, Okawa K, Iwamatsu A, Kaibuchi K.** Regulation of myosin phosphatase by Rho and Rho-associated kinase (Rho-kinase). *Science* 273: 245–248, 1996.
54. **Kishi H, Bao J, Kohama K.** Inhibitory effects of ML-9, wortmannin, and Y-27632 on the chemotaxis of vascular smooth muscle cells in response to platelet-derived growth factor-BB. *J Biochem* 128: 719–722, 2000.
55. **Kishi T, Hirooka Y, Masumoto A, Ito K, Kimura Y, Inokuchi K, Tagawa T, Shimokawa H, Takeshita A, Sunagawa K.** Rho-kinase inhibitor improves increased vascular resistance and impaired vasodilation of the forearm in patients with heart failure. *Circulation* 111: 2741–2747, 2005.
56. **Komander D, Garg R, Wan PT, Ridley AJ, Barford D.** Mechanism of multi-site phosphorylation from a ROCK-I:RhoE complex structure. *EMBO J* 27: 3175–3185, 2008.
57. **Kunieda T, Minamino T, Nishi J, Tateno K, Oyama T, Katsuno T, Miyauchi H, Orimo M, Okada S, Takamura M, Nagai T, Kaneko S, Komuro I.** Angiotensin II induces premature senescence of vascular smooth muscle cells and accelerates the development of atherosclerosis via a p21-dependent pathway. *Circulation* 114: 953–960, 2006.

58. **Leung T, Manser E, Tan L, Lim L.** A novel serine/threonine kinase binding the Ras-related RhoA GTPase which translocates the kinase to peripheral membranes. *J Biol Chem* 270: 29051–29054, 1995.
59. **Li M, Fukagawa NK.** Age-related changes in redox signaling and VSMC function. *Antioxid Redox Signal* 12: 641–655.
60. **Liao DF, Jin ZG, Baas AS, Daum G, Gygi SP, Aebersold R, Berk BC.** Purification and identification of secreted oxidative stress-induced factors from vascular smooth muscle cells. *J Biol Chem* 275: 189–196, 2000.
61. **Liao JK, Seto M, Noma K.** Rho kinase (ROCK) inhibitors. *J Cardiovasc Pharmacol* 50: 17–24, 2007.
62. **Libby P.** Inflammation in atherosclerosis. *Nature* 420: 868–874, 2002.
63. **Libby P, Okamoto Y, Rocha VZ, Folco E.** Inflammation in atherosclerosis: transition from theory to practice. *Circ J* 74: 213–220, 2010.
64. **Loirand G, Guerin P, Pacaud P.** Rho kinases in cardiovascular physiology and pathophysiology. *Circ Res* 98: 322–334, 2006.
65. **Loirand G, Pacaud P.** The role of Rho protein signaling in hypertension. *Nat Rev Cardiol* 7: 637–647, 2010.
66. **Mackay DJ, Hall A.** Rho GTPases. *J Biol Chem* 273: 20685–20688, 1998.
67. **Manning MW, Cassis LA, Daugherty A.** Differential effects of doxycycline, a broad-spectrum matrix metalloproteinase inhibitor, on angiotensin II-induced atherosclerosis and abdominal aortic aneurysms. *Arterioscler Thromb Vasc Biol* 23: 483–488, 2003.
68. **Masumoto A, Mohri M, Shimokawa H, Urakami L, Usui M, Takeshita A.** Suppression of coronary artery spasm by the Rho-kinase inhibitor fasudil in patients with vasospastic angina. *Circulation* 105: 1545–1547, 2002.
69. **Matsui T, Amano M, Yamamoto T, Chihara K, Nakafuku M, Ito M, Nakano T, Okawa K, Iwamatsu A, Kaibuchi K.** Rho-associated kinase, a novel serine/threonine kinase, as a putative target for small GTP binding protein Rho. *EMBO J* 15: 2208–2216, 1996.
70. **Matsumoto Y, Uwatoku T, Oi K, Abe K, Hattori T, Morishige K, Eto Y, Fukumoto Y, Nakamura K, Shibata Y, Matsuda T, Takeshita A, Shimokawa H.** Long-term inhibition of Rho-kinase suppresses neointimal formation after stent implantation in porcine coronary arteries: involvement of multiple mechanisms. *Arterioscler Thromb Vasc Biol* 24: 181–186, 2004.
71. **Mehta PK, Griendling KK.** Angiotensin II cell signaling: physiological and pathological effects in the cardiovascular system. *Am J Physiol Cell Physiol* 292: C82–C97, 2007.
72. **Miyata K, Shimokawa H, Kandabashi T, Higo T, Morishige K, Eto Y, Egashira K, Kaibuchi K, Takeshita A.** Rho-kinase is involved in macrophage-mediated formation of coronary vascular lesions in pigs in vivo. *Arterioscler Thromb Vasc Biol* 20: 2351–2358, 2000.
73. **Mohri M, Shimokawa H, Hirakawa Y, Masumoto A, Takeshita A.** Rho-kinase inhibition with intracoronary fasudil prevents myocardial ischemia in patients with coronary microvascular spasm. *J Am Coll Cardiol* 41: 15–19, 2003.
74. **Mukai Y, Shimokawa H, Matoba T, Kandabashi T, Satoh S, Hiroki J, Kaibuchi K, Takeshita A.** Involvement of Rho-kinase in hypertensive vascular disease: a novel therapeutic target in hypertension. *FASEB J* 15: 1062–1064, 2001.
75. **Nakagawa O, Fujisawa K, Ishizaki T, Saito Y, Nakao K, Narumiya S.** ROCK-I and ROCK-II, two isoforms of Rho-associated coiled-coil forming protein serine/threonine kinase in mice. *FEBS Lett* 392: 189–193, 1996.
76. **Nakamura K, Fushimi K, Kouchi H, Mihara K, Miyazaki M, Ohe T, Namba M.** Inhibitory effects of antioxidants on neonatal rat cardiac myocyte hypertrophy induced by tumor necrosis factor-alpha and angiotensin II. *Circulation* 98: 794–799, 1998.
77. **Neco P, Giner D, Viniegra S, Borges R, Villarroel A, Gutierrez LM.** New roles of myosin II during vesicle transport and fusion in chromaffin cells. *J Biol Chem* 279: 27450–27457, 2004.
78. **Nigro P, Satoh K, O'Dell MR, Soe NN, Cui Z, Mohan A, Abe J, Alexis JD, Sparks JD, Berk BC.** Cyclophilin A is an inflammatory mediator that promotes atherosclerosis in apolipoprotein E-deficient mice. *J Exp Med* 208: 53–66, 2011.
79. **Noma K, Rikitake Y, Oyama N, Yan G, Alcaide P, Liu PY, Wang H, Ahl D, Sawada N, Okamoto R, Hiroi Y, Shimizu K, Luscinskas FW, Sun J, Liao JK.** ROCK1 mediates leukocyte recruitment and neointima formation following vascular injury. *J Clin Invest* 118: 1632–1644, 2008.
80. **Oi K, Shimokawa H, Hiroki J, Uwatoku T, Abe K, Matsumoto Y, Nakajima Y, Nakajima K, Takeichi S, Takeshita A.** Remnant lipoproteins from patients with sudden cardiac death enhance coronary vasospastic activity through upregulation of Rho-kinase. *Arterioscler Thromb Vasc Biol* 24: 918–922, 2004.
81. **Olofsson B.** Rho guanine dissociation inhibitors: pivotal molecules in cellular signalling. *Cell Signal* 11: 545–554, 1999.
82. **Omar HA, Cherry PD, Mortelliti MP, Burke-Wolin T, Wolin MS.** Inhibition of coronary artery superoxide dismutase attenuates endothelium-dependent and -independent nitrovasodilator relaxation. *Circ Res* 69: 601–608, 1991.
83. **Radeff JM, Nagy Z, Stern PH.** Rho and Rho kinase are involved in parathyroid hormone-stimulated protein kinase C alpha translocation and IL-6 promoter activity in osteoblastic cells. *J Bone Miner Res* 19: 1882–1891, 2004.
84. **Rao GN, Berk BC.** Active oxygen species stimulate vascular smooth muscle cell growth and proto-oncogene expression. *Circ Res* 70: 593–599, 1992.
85. **Riento K, Guasch RM, Garg R, Jin B, Ridley AJ.** RhoE binds to ROCK I and inhibits downstream signaling. *Mol Cell Biol* 23: 4219–4229, 2003.
86. **Riento K, Ridley AJ.** Rocks: multifunctional kinases in cell behaviour. *Nat Rev Mol Cell Biol* 4: 446–456, 2003.
87. **Ross R.** Atherosclerosis is an inflammatory disease. *Am Heart J* 138: S419–S420, 1999.
88. **Sadoshima J, Xu Y, Slayter HS, Izumo S.** Autocrine release of angiotensin II mediates stretch-induced hypertrophy of cardiac myocytes in vitro. *Cell* 75: 977–984, 1993.
89. **Sato S, Ikegaki I, Asano T, Shimokawa H.** Antiischemic properties of fasudil in experimental models of vasospastic angina. *Jpn J Pharmacol* 87: 34–40, 2001.
90. **Satoh K, Fukumoto Y, Nakano M, Sugimura K, Nawata J, Demachi J, Karibe A, Kagaya Y, Ishii N, Sugamura K, Shimokawa H.** Statin ameliorates hypoxia-induced pulmonary hypertension associated with down-regulated stromal cell-derived factor-1. *Cardiovasc Res* 81: 226–234, 2009.
91. **Satoh K, Fukumoto Y, Sugimura K, Tatebe S, Miura Y, Miyamichi S, Nakamura K, Nigro P, Berk BC, Shimokawa H.** Cyclophilin A mediates pulmonary vascular remodeling by rho-kinase activation in patients with pulmonary hypertension. *Circulation* 122, *Suppl*: A11001, 2010.
92. **Satoh K, Kagaya Y, Nakano M, Ito Y, Ohta J, Tada H, Karibe A, Minegishi N, Suzuki N, Yamamoto M, Ono M, Watanabe J, Shirato K, Ishii N, Sugamura K, Shimokawa H.** Important role of endogenous erythropoietin system in recruitment of endothelial progenitor cells in hypoxia-induced pulmonary hypertension in mice. *Circulation* 113: 1442–1450, 2006.
93. **Satoh K, Matoba T, Suzuki J, O'Dell MR, Nigro P, Cui Z, Mohan A, Pan S, Li L, Jin ZG, Yan C, Abe J, Berk BC.** Cyclophilin A mediates vascular remodeling by promoting inflammation and vascular smooth muscle cell proliferation. *Circulation* 117: 3088–3098, 2008.
94. **Satoh K, Nigro P, Berk BC.** Oxidative stress and vascular smooth muscle cell growth: a mechanistic linkage by cyclophilin A. *Antioxid Redox Signal* 12: 675–682, 2010.
95. **Satoh K, Nigro P, Matoba T, O'Dell MR, Cui Z, Shi X, Mohan A, Yan C, Abe J, Illig KA, Berk BC.** Cyclophilin A enhances vascular oxidative stress and the development of angiotensin II-induced aortic aneurysms. *Nat Med* 15: 649–656, 2009.
96. **Satoh K, Nigro P, Zeidan A, Soe NN, Jaffre F, Oikawa M, O'Dell MR, Cui Z, Menon P, Lu Y, Mohan A, Yan C, Blaxall BC, Berk BC.** Cyclophilin A promotes cardiac hypertrophy in apolipoprotein e-deficient mice. *Arterioscler Thromb Vasc Biol* 31: 1116–1123, 2011.
97. **Satoh K, Shimokawa H, Berk BC.** Cyclophilin A: promising new target in cardiovascular therapy. *Circ J* 74: 2249–2256, 2010.
98. **Satoh S, Ikegaki I, Toshima Y, Watanabe A, Asano T, Shimokawa H.** Effects of Rho-kinase inhibitor on vasopressin-induced chronic myocardial damage in rats. *Life Sci* 72: 103–112, 2002.
99. **Sauzeau V, Le Jeune H, Cario-Toumaniantz C, Vaillant N, Gadeau AP, Desgranges C, Scalbert E, Chardin P, Pacaud P, Loirand G.** $P2Y_1$, $P2Y_2$, $P2Y_4$, and $P2Y_6$ receptors are coupled to Rho and Rho kinase activation in vascular myocytes. *Am J Physiol Heart Circ Physiol* 278: H1751–H1761, 2000.
100. **Sauzeau V, Le Mellionnec E, Bertoglio J, Scalbert E, Pacaud P, Loirand G.** Human urotensin II-induced contraction and arterial smooth muscle cell proliferation are mediated by RhoA and Rho-kinase. *Circ Res* 88: 1102–1104, 2001.

101. **Sawada N, Itoh H, Ueyama K, Yamashita J, Doi K, Chun TH, Inoue M, Masatsugu K, Saito T, Fukunaga Y, Sakaguchi S, Arai H, Ohno N, Komeda M, Nakao K.** Inhibition of rho-associated kinase results in suppression of neointimal formation of balloon-injured arteries. *Circulation* 101: 2030–2033, 2000.
102. **Schmidt A, Hall A.** Guanine nucleotide exchange factors for Rho GTPases: turning on the switch. *Genes Dev* 16: 1587–1609, 2002.
103. **Seasholtz TM, Majumdar M, Kaplan DD, Brown JH.** Rho and Rho kinase mediate thrombin-stimulated vascular smooth muscle cell DNA synthesis and migration. *Circ Res* 84: 1186–1193, 1999.
104. **Sebbagh M, Hamelin J, Bertoglio J, Solary E, Breard J.** Direct cleavage of ROCK II by granzyme B induces target cell membrane blebbing in a caspase-independent manner. *J Exp Med* 201: 465–471, 2005.
105. **Shibata R, Kai H, Seki Y, Kato S, Morimatsu M, Kaibuchi K, Imaizumi T.** Role of Rho-associated kinase in neointima formation after vascular injury. *Circulation* 103: 284–289, 2001.
106. **Shibata R, Ouchi N, Murohara T.** Adiponectin and cardiovascular disease. *Circ J* 73: 608–614, 2009.
107. **Shimizu T, Satoh K, Tanaka S, Fukumoto Y, Shimokawa H.** ROCK2 in vascular smooth muscle cells plays a crucial role for hypoxia-induced pulmonary hypertension in mice (Abstract). *Circulation* 122: A16516, 2010.
108. **Shimizu Y, Thumkeo D, Keel J, Ishizaki T, Oshima H, Oshima M, Noda Y, Matsumura F, Taketo MM, Narumiya S.** ROCK-I regulates closure of the eyelids and ventral body wall by inducing assembly of actomyosin bundles. *J Cell Biol* 168: 941–953, 2005.
109. **Shimokawa H.** Cellular and molecular mechanisms of coronary artery spasm: lessons from animal models. *Jpn Circ J* 64: 1–12, 2000.
110. **Shimokawa H.** Primary endothelial dysfunction: atherosclerosis. *J Mol Cell Cardiol* 31: 23–37, 1999.
111. **Shimokawa H.** Rho-kinase as a novel therapeutic target in treatment of cardiovascular diseases. *J Cardiovasc Pharmacol* 39: 319–327, 2002.
112. **Shimokawa H, Hiramori K, Iinuma H, Hosoda S, Kishida H, Osada H, Katagiri T, Yamauchi K, Yui Y, Minamino T, Nakashima M, Kato K.** Anti-anginal effect of fasudil, a Rho-kinase inhibitor, in patients with stable effort angina: a multicenter study. *J Cardiovasc Pharmacol* 40: 751–761, 2002.
113. **Shimokawa H, Ito A, Fukumoto Y, Kadokami T, Nakaike R, Sakata M, Takayanagi T, Egashira K, Takeshita A.** Chronic treatment with interleukin-1 beta induces coronary intimal lesions and vasospastic responses in pigs in vivo. The role of platelet-derived growth factor. *J Clin Invest* 97: 769–776, 1996.
114. **Shimokawa H, Morishige K, Miyata K, Kandabashi T, Eto Y, Ikegaki I, Asano T, Kaibuchi K, Takeshita A.** Long-term inhibition of Rho-kinase induces a regression of arteriosclerotic coronary lesions in a porcine model in vivo. *Cardiovasc Res* 51: 169–177, 2001.
115. **Shimokawa H, Rashid M.** Development of Rho-kinase inhibitors for cardiovascular medicine. *Trends Pharmacol Sci* 28: 296–302, 2007.
116. **Shimokawa H, Seto M, Katsumata N, Amano M, Kozai T, Yamawaki T, Kuwata K, Kandabashi T, Egashira K, Ikegaki I, Asano T, Kaibuchi K, Takeshita A.** Rho-kinase-mediated pathway induces enhanced myosin light chain phosphorylations in a swine model of coronary artery spasm. *Cardiovasc Res* 43: 1029–1039, 1999.
117. **Shimokawa H, Takeshita A.** Rho-kinase is an important therapeutic target in cardiovascular medicine. *Arterioscler Thromb Vasc Biol* 25: 1767–1775, 2005.
118. **Shimokawa H, Tomoike H, Nabeyama S, Yamamoto H, Araki H, Nakamura M, Ishii Y, Tanaka K.** Coronary artery spasm induced in atherosclerotic miniature swine. *Science* 221: 560–562, 1983.
119. **Sun J, Sukhova GK, Yang M, Wolters PJ, MacFarlane LA, Libby P, Sun C, Zhang Y, Liu J, Ennis TL, Knispel R, Xiong W, Thompson RW, Baxter BT, Shi GP.** Mast cells modulate the pathogenesis of elastase-induced abdominal aortic aneurysms in mice. *J Clin Invest* 117: 3359–3368, 2007.
120. **Suzuki J, Jin ZG, Meoli DF, Matoba T, Berk BC.** Cyclophilin A is secreted by a vesicular pathway in vascular smooth muscle cells. *Circ Res* 98: 811–817, 2006.
121. **Takagi Y, Yasuda S, Takahashi J, Takeda M, Nakayama M, Ito K, Hirose M, Wakayama Y, Fukuda K, Shimokawa H.** Importance of dual induction tests for coronary vasospasm and ventricular fibrillation in patients surviving out-of-hospital cardiac arrest. *Circ J* 73: 767–769, 2009.
122. **Takai Y, Sasaki T, Matozaki T.** Small GTP-binding proteins. *Physiol Rev* 81: 153–208, 2001.
123. **Takeda K, Ichiki T, Tokunou T, Iino N, Fujii S, Kitabatake A, Shimokawa H, Takeshita A.** Critical role of Rho-kinase and MEK/ERK pathways for angiotensin II-induced plasminogen activator inhibitor type-1 gene expression. *Arterioscler Thromb Vasc Biol* 21: 868–873, 2001.
124. **Takemoto M, Liao JK.** Pleiotropic effects of 3-hydroxy-3-methylglutaryl coenzyme a reductase inhibitors. *Arterioscler Thromb Vasc Biol* 21: 1712–1719, 2001.
125. **Takemoto M, Sun J, Hiroki J, Shimokawa H, Liao JK.** Rho-kinase mediates hypoxia-induced downregulation of endothelial nitric oxide synthase. *Circulation* 106: 57–62, 2002.
126. **Takimoto E, Kass DA.** Role of oxidative stress in cardiac hypertrophy and remodeling. *Hypertension* 49: 241–248, 2007.
127. **Taniyama Y, Griendling KK.** Reactive oxygen species in the vasculature: molecular and cellular mechanisms. *Hypertension* 42: 1075–1081, 2003.
128. **Thomas M, Gavrila D, McCormick ML, Miller FJ ,Jr, Daugherty A, Cassis LA, Dellsperger KC, Weintraub NL.** Deletion of p47phox attenuates angiotensin II-induced abdominal aortic aneurysm formation in apolipoprotein E-deficient mice. *Circulation* 114: 404–413, 2006.
129. **Thompson RW, Baxter BT.** MMP inhibition in abdominal aortic aneurysms. Rationale for a prospective randomized clinical trial. *Ann NY Acad Sci* 878: 159–178, 1999.
130. **Thumkeo D, Keel J, Ishizaki T, Hirose M, Nonomura K, Oshima H, Oshima M, Taketo MM, Narumiya S.** Targeted disruption of the mouse rho-associated kinase 2 gene results in intrauterine growth retardation and fetal death. *Mol Cell Biol* 23: 5043–5055, 2003.
131. **Uehata M, Ishizaki T, Satoh H, Ono T, Kawahara T, Morishita T, Tamakawa H, Yamagami K, Inui J, Maekawa M, Narumiya S.** Calcium sensitization of smooth muscle mediated by a Rho-associated protein kinase in hypertension. *Nature* 389: 990–994, 1997.
132. **Utsunomiya T, Satoh S, Ikegaki I, Toshima Y, Asano T, Shimokawa H.** Antianginal effects of hydroxyfasudil, a Rho-kinase inhibitor, in a canine model of effort angina. *Br J Pharmacol* 134: 1724–1730, 2001.
133. **Vahebi S, Kobayashi T, Warren CM, de Tombe PP, Solaro RJ.** Functional effects of rho-kinase-dependent phosphorylation of specific sites on cardiac troponin. *Circ Res* 96: 740–747, 2005.
134. **van Nieuw Amerongen GP, van Delft S, Vermeer MA, Collard JG, van Hinsbergh VW.** Activation of RhoA by thrombin in endothelial hyperpermeability: role of Rho kinase and protein tyrosine kinases. *Circ Res* 87: 335–340, 2000.
135. **Vanhoutte PM.** Endothelium-derived free radicals: for worse and for better. *J Clin Invest* 107: 23–25, 2001.
136. **Wang F, Okamoto Y, Inoki I, Yoshioka K, Du W, Qi X, Takuwa N, Gonda K, Yamamoto Y, Ohkawa R, Nishiuchi T, Sugimoto N, Yatomi Y, Mitsumori K, Asano M, Kinoshita M, Takuwa Y.** Sphingosine-1-phosphate receptor-2 deficiency leads to inhibition of macrophage proinflammatory activities and atherosclerosis in apoE-deficient mice. *J Clin Invest* 120: 3979–3995, 2010.
137. **Wang J, Weigand L, Foxson J, Shimoda LA, Sylvester JT.** Ca^{2+} signaling in hypoxic pulmonary vasoconstriction: effects of myosin light chain and Rho kinase antagonists. *Am J Physiol Lung Cell Mol Physiol* 293: L674–L685, 2007.
138. **Wang L, Wang CH, Jia JF, Ma XK, Li Y, Zhu HB, Tang H, Chen ZN, Zhu P.** Contribution of cyclophilin A to the regulation of inflammatory processes in rheumatoid arthritis. *J Clin Immunol* 30: 24–33, 2010.
139. **Wang Y, Zheng XR, Riddick N, Bryden M, Baur W, Zhang X, Surks HK.** ROCK isoform regulation of myosin phosphatase and contractility in vascular smooth muscle cells. *Circ Res* 104: 531–540, 2009.
140. **Wang YX, Martin-McNulty B, da Cunha V, Vincelette J, Lu X, Feng Q, Halks-Miller M, Mahmoudi M, Schroeder M, Subramanyam B, Tseng JL, Deng GD, Schirm S, Johns A, Kauser K, Dole WP, Light DR.** Fasudil, a Rho-kinase inhibitor, attenuates angiotensin II-induced abdominal aortic aneurysm in apolipoprotein E-deficient mice by inhibiting apoptosis and proteolysis. *Circulation* 111: 2219–2226, 2005.
141. **Weintraub NL.** Understanding abdominal aortic aneurysm. *N Engl J Med* 361: 1114–1116, 2009.
142. **Yada T, Shimokawa H, Hiramatsu O, Kajita T, Shigeto F, Tanaka E, Shinozaki Y, Mori H, Kiyooka T, Katsura M, Ohkuma S, Goto M, Ogasawara Y, Kajiya F.** Beneficial effect of hydroxyfasudil, a

specific Rho-kinase inhibitor, on ischemia/reperfusion injury in canine coronary microcirculation in vivo. *J Am Coll Cardiol* 45: 599–607, 2005.

143. **Yamakawa T, Tanaka S, Numaguchi K, Yamakawa Y, Motley ED, Ichihara S, Inagami T.** Involvement of Rho-kinase in angiotensin II-induced hypertrophy of rat vascular smooth muscle cells. *Hypertension* 35: 313–318, 2000.
144. **Yang Y, Lu N, Zhou J, Chen ZN, Zhu P.** Cyclophilin A up-regulates MMP-9 expression and adhesion of monocytes/macrophages via CD147 signalling pathway in rheumatoid arthritis. *Rheumatology (Oxford)* 47: 1299–1310, 2008.
145. **Yoshimura K, Aoki H, Ikeda Y, Fujii K, Akiyama N, Furutani A, Hoshii Y, Tanaka N, Ricci R, Ishihara T, Esato K, Hamano K, Matsuzaki M.** Regression of abdominal aortic aneurysm by inhibition of c-Jun N-terminal kinase. *Nat Med* 11: 1330–1338, 2005.
146. **Zhou Q, Gensch C, Liao JK.** Rho-associated coiled-coil-forming kinases (ROCKs): potential targets for the treatment of atherosclerosis and vascular disease. *Trends Pharmacol Sci* 32: 167–173, 2011.

Rabieyousefi et al. BMC Immunology 2011, 12:67
http://www.biomedcentral.com/1471-2172/12/67

BMC Immunology

RESEARCH ARTICLE Open Access

Indispensable roles of OX40L-derived signal and epistatic genetic effect in immune-mediated pathogenesis of spontaneous pulmonary hypertension

Moloud Rabieyousefi[1], Pejman Soroosh[2,7*], Kimio Satoh[3], Fumiko Date[1], Naoto Ishii[2,6], Masahiro Yamashita[1], Masahiko Oka[4], Ivan F McMurtry[4], Hiroaki Shimokawa[3], Masato Nose[5], Kazuo Sugamura[2] and Masao Ono[1,6*]

Abstract

Background: Pulmonary hypertension (PH) refers to a spectrum of diseases with elevated pulmonary artery pressure. Pulmonary arterial hypertension (PAH) is a disease category that clinically presents with severe PH and that is histopathologically characterized by the occlusion of pulmonary arterioles, medial muscular hypertrophy, and/or intimal fibrosis. PAH occurs with a secondary as well as a primary onset. Secondary PAH is known to be complicated with immunological disorders. The aim of the present study is to histopathologically and genetically characterize a new animal model of PAH and clarify the role of OX40 ligand in the pathogenesis of PAH.

Results: Spontaneous onset of PAH was stably identified in mice with immune abnormality because of overexpression of the tumor necrosis factor (TNF) family molecule OX40 ligand (OX40L). Histopathological and physical examinations revealed the onset of PAH-like disorders in the C57BL/6 (B6) strain of OX40L transgenic mice (B6.TgL). Comparative analysis performed using different strains of transgenic mice showed that this onset depends on the presence of OX40L in the B6 genetic background. Genetic analyses demonstrated a susceptibility locus of a B6 allele to this onset on chromosome 5. Immunological analyses revealed that the excessive OX40 signals in TgL mice attenuates expansion of regulatory T cells the B6 genetic background, suggesting an impact of the B6 genetic background on the differentiation of regulatory T cells.

Conclusion: Present findings suggest a role for the OX40L-derived immune response and epistatic genetic effect in immune-mediated pathogenesis of PAH.

Background

Pulmonary hypertension (PH) is a severe disease condition that can lead to progressive right ventricular failure and ultimately to death. Pulmonary arterial hypertension (PAH) is a major class of PH defined in the classification of the World Health Organization (WHO). The main histopathological manifestations of PAH are vasoconstriction, endothelial cell proliferation and fibrosis, smooth-muscle cell proliferation, and thrombosis in small pulmonary arteries. These changes result in elevation of pulmonary vascular resistance and, consequently, in pulmonary arterial pressure [1].

PAH occurs as either a primary (idiopathic or familial) or a secondary disease. According to the WHO classification, inflammatory conditions, such as collagen vascular diseases, and viral infections are associated with the occurrence of PAH. Indeed, patients with a subset of idiopathic PAH have some inflammatory disturbances, presented as elevated circulating levels of TNF-α, interleukin (IL)-1, and IL-6 [2]. In the case of severe PAH in humans, infiltration of immune cells, including T cells, B cells, and macrophages, is occasionally observed in pulmonary vascular lesions [3]. Most of the $CD4^+$ and $CD8^+$ T cells infiltrating into the intimal lesions have been

* Correspondence: psoroosh@its.jnj.com; onomasao@med.tohoku.ac.jp
[1]Department of Pathology, Tohoku University Graduate School of Medicine, 2-1 Seiryo, Aoba-ku, Sendai, Miyagi 980-8575 Japan
[2]Department of Immunology, Tohoku University Graduate School of Medicine, 2-1 Seiryo, Aoba-ku, Sendai, Miyagi 980-8575 Japan
Full list of author information is available at the end of the article

shown to express effector memory T-cell markers, indicating the active status of the T cells. In animal models, augmented expression of IL-18 or administration of IL-6 is sufficient to induce mild spontaneous PH [4,5]. In the former case, IL-13 has been shown to critically mediate inflammatory signals in the lung. Recent studies have proposed that naturally arising $CD4^+CD25^+$ regulatory T (T_{reg}) cells, or their mediators, may inhibit the development of experimental PH [6]. Furthermore, it has been suggested that the deficiency of $CD4^+$ T cells in humans (e.g., in cases of HIV infection), or the depletion of $CD4^+$ T cells in experimental animal models, is associated with the development of PAH [7]. These observations implicate an immune-mediated mechanism in the development of PAH.

Signals through T-cell costimulatory molecules are critically involved in eliciting optimal T-cell functions [8]. OX40 (TNFRSF4, CD134) is a member of the TNF receptor superfamily that is transiently expressed on activated T cells. The ligand of OX40 (OX40L: TNFSF4, CD134L) is mainly expressed on mature antigen-presenting cells as well as on vascular endothelial cells [9-12]. The OX40-OX40L interaction is required for optimal effector function of T cells [13,14] and generation of memory T cells [15-18]. Recently, growing evidence has unveiled the importance of OX40 signals in the accumulation of effector $CD4^+$ T cells at inflammation sites in mouse models of autoimmune diseases. Moreover, a recent study has demonstrated that constitutive OX40-OX40L interactions in OX40L transgenic mice entail spontaneous development of ulcerative colitis-like disease and an undetermined lung disease, which is accompanied by significant production of an anti-DNA antibody [19]. Interestingly, these pathological manifestations have been observed in mice with the C57BL/6 (B6) genetic background but not in those with the BALB/c (BALB) genetic background. The strain-specific pathological manifestations implicate the presence of a genetic predisposition that modulates OX40L-dependent inflammation in the colon and lungs.

The goal of this study was to characterize the undetermined lung disease presented in an OX40L-transgenic B6 strain (B6.TgL) of mice. In the present study, we proposed a new spontaneous model for PAH. Furthermore, this study provided novel insight into the role of the OX40L-derived signal and the genetic predisposition in the immune-mediated pathogenic mechanism of PAH.

Methods

Mice

Mice with OX40L transgene under the expression control of *lck* promoter were generated in a C57BL/6 genetic background as described previously (B6.TgL) [19]. To generate OX40L transgenic mice on BALB/c background (BALB.TgL), B6.TgL backcrossed to BALB/c strains more than 8 times. Age and sex-matched wild-type C57BL/6 and BALB/c were used as controls. For genetic analyses, TgL mice with mixed genetic background were prepared by the mating of BALB × B6.TgL and (BALB × B6) F1 × B6.TgL. All mice were bred and maintained in conventional clean room in the animal department of the Oriental Bio-service, Co. Ltd, Shizuoka, Japan. In all animal experiments in this study, we followed the Tohoku University guidelines for animal experimentation.

Histopathological examinations

At 20 weeks of age, each mouse was killed under ether anesthesia. The whole lung was immersion fixed in 10% formalin in 0.01 M phosphate buffer (pH 7.2), and embedded in paraffin. Tissue sections were stained with hematoxylin and eosin (H&E) and Masson's trichrome for light-microscopic examination. The disease score of PAH was histopathologically determined. Ten small pulmonary arteries along with terminal bronchioles were individually graded under microscopic examination according to following histopathological criteria: 0, normal; 1, significant, slight thickening of the media; 2, thickening of the media with intimal (endothelial) proliferation and/or fibrosis. A mean grade of all points examined was considered as an individual PAH score. Immunohistochemical analyses were performed using the primary antibodies to human α-smooth muscle actin (αSMA) (DACO, Tokyo, Japan), which has been shown to react mouse αSMA, and mouse CD31 (Santa Cruz Biotechnology, Santa Cruz, CA).

Right ventricular systolic pressure measurements

B6, BALB, B6.TgL, and BALB.TgL mice were anesthetized by intraperitoneal injection of ketamine hydrochloride (60 mg/kg) and xylazine (8 mg/kg) or, in the second series of measurement using B6, and BALB.TgL mice, pentobarbital sodium (50 mg/kg). Right ventricular systolic pressure (RVSP) was measured in spontaneously breathing mice by direct puncture of the right ventricle with a 25-gauge needle connected to a pressure transducer [20]. In the second series with the pentobarbital anesthetization, it was measured in artificially ventilated mice with median thoracotomy.

Evaluation of right ventricular hypertrophy

The hearts isolated from B6, BALB, B6.TgL, and BALB.TgL mice were fixed in formalin and dissected into right ventricle (RV), left ventricle (LV), and interventricular septum (IVS). The dissected ventricles were carefully washed in saline to remove blood clots and separately weighted. Right ventricular hypertrophy was evaluated by the weight ratio of RV/(LV+IVS).

Antibodies and flow cytometric analysis

Anti-CD3-FITC, anti-CD4-allophycocyanin, anti-CD25-allophycocyanin, anti-CD44-phycoerythrin (PE), anti-CD62L-FITC, and anti-IL-17-PE were purchased from BD Biosciences (San Diego, CA). Anti-mouse Foxp3-PE (FJK-16S) was purchased from eBioscience (San Diego, CA). Anti-mouse CD3ε (clone 2C11) used for T cell stimulation and anti-mouse CD16/32 (clone 2.4G2) used for Fc receptor blocking were purified from hybridoma-cultured supernatants in our laboratory. Cells were incubated with antibodies for 30 min at 4°C and then washed to remove unbound antibodies. All the samples were analyzed with a FACSCalibur™ flow cytometer and the CellQuest™ program (BD Biosciences).

Preparation of lymphocyte culture and cytokine measurements

Single-cell suspensions were prepared from spleen and lungs of an 8 to 10 week-old mouse, in which the lung disease of interest is not developed. Lymphocytes in the lung were obtained by digesting minced lung tissues with 150 U/ml collagenase (Maeda Co. Ltd., Tokyo, Japan) as described previously [21]. The number of effector/memory and regulatory T cells were calculated based on the percentage of each subpopulation that was $CD44^{high}CD62L^{low}$ and $CD4^{+}Foxp3^{+}$, respectively, and the total cell number in each organ. Total lymphocytes isolated from lung tissues that contained equal number of effector/memory $CD4^{+}$T cells (normalized based on absolute number of effector/memory CD4 T cells) were stimulated with soluble anti-CD3ε (10 μg/ml) at 37°C for the indicated time. IL-13 levels were assayed in cultured supernatants using ELISA kit for IL-13 (R&D Systems, Minneapolis, MN), according to the manufacturer's recommendations. The production of IL-17 in lymphocytes was detected by intracellular staining with anti-IL-17-PE following incubation of lymphocytes for 4 h with 50 ng/ml PMA, 500 ng/ml Ionomycin (Sigma-Aldrich, St. Louis, MO) in the presence of 10 μg/ml brefeldin A (Invitrogen, Carlsbad, CA).

Genetic mapping

Genotypes of BCN2.TgL mice were determined by polymerase chain reaction (PCR) using genomic DNA prepared from the tail tip. The genotyping PCR was performed using standard reagent and the following conditions: 94°C for 5 min, 35 cycle of 94°C for 30 sec, 58°C for 30 sec, 72°C for 30 sec, and final extension 72°C for 5 min with the 98 microsatellite markers (additional file 1), which represent amplified fragment-length polymorphism between BALB and B6 strains. This genotyping provided full coverage of the mouse autosomes with the marker spaced an average of 12.5 cM apart and a maximum distance of 35 cM between any two markers. PCR products were visualized with electrophoresis on 2-4% agarose gels containing 0.01% ethidium bromide.

In a genome-wide scan, we determined genotypes of the 48 BCN2.TgL mice, which were selected as the top (severest) 24 and the bottom 24 on the list of PAH score, at all the 98 microsatellite positions (additional file 1) . The association at each microsatellite position was evaluated with chi-square test for independence between the genotypes and the two groups that were positive and negative for the incidence of PAH, using standard 2 × 2 contingency matrices. A p value less than 0.05 was regarded as suggestive association. The suggestive association was confirmed by the two-tail t-test for the difference of means between the two genotype groups of a total of 341 BCN2.TgL mice. In this test a P value less than 0.0034 was regarded as suggestive association. This P threshold was referred to the previous recommendation [22].

In a linkage mapping, a linkage position was determined with the quantitative trait locus (QTL) program. The logarithm of odd (LOD) was determined with the interval mapping program in the Windows QTL Cartographer (V2.5) software. The PAH scores of all BCN2.TgL mice were used as an indicator of phenotype. A suggestively significant level (α = 0.05) of LOD was determined by the permutation test installed in this software (1000 permutations). Map positions (cM) of the microsatellite makers were based on the information of the Mouse Genome Database of The Jackson Laboratory (http://www.informatics.jax.org).

Statistics

A 95% confidence interval shown in Table 1 was calculated using the method described previously [23]. The two-tailed t-test was used to evaluate a difference of

Table 1 Summary of PAH scores of B6, BALB, and transgenic strains of mice

Mice*		n†	Median of score	95% CI‡	Statistics§
B6		9	0	0 - 0.1	
BALB		2	0	n.d.	
B6. TgL		15	0.7	0.35 - 1.05	¶
BALB. TgL		8	0	0 - 0.1	
BCF1. TgL		30	0.05	0 - 0.1	
BCN2. TgL	female	174	0.25	0.2 - 0.4	¶
BCN2. TgL	male	167	0.25	0.2 - 0.4	¶

* All mice were killed at 20 week-old for this examination. BCF1, BALB × B6; BCN2, BCF1 × B6.TgL.

† Number of mice tested.

‡ CI, confidential interval. The CI was not determined (n.d.) for BALB/c (BALB).

§ The significance of this study was evaluated by Mann-Whitney U-test for the all strains.

¶, P < 0.01 (v.s. B6).

means between two groups. A P value less than 0.05 considered as significant.

Results

Histopathological characterization of the lung phenotype

Microscopic examination revealed diffuse pathological changes in the small- to medium-sized pulmonary arteries in B6.TgL (Figure 1A, E), but not in B6 (Figure 1B), BALB strain of OX40L transgenic mice (BALB.TgL) (Figure 1C), or BALB (Figure 1D). This vascular lesion was found to be readily accompanied with perivascular infiltration of lymphocytes and, to a lesser extent, neutrophils (Figure 1F). These changes were mainly observed in arteries contained in bronchovascular bundles (respiratory arteries) and were typically characterized by fibrocellular endothelial proliferation of the intimal layer and, to a lesser extent, medial muscular hypertrophy (Figure 1G and 1H). Neither muscularization of distal pulmonary arterioles, which is a common pathological change in a hypoxic PAH model, nor plexiform lesions, found in human PAH, were identified. The cells in the intimal lesion were characterized as positive for a myofibroblast marker, smooth muscle-specific actin (αSMA) (Figure 1I), and an endothelial cell marker, CD31 (Figure 1J). When no treatment was administered to avoid vasospasm before the histopathological preparation, vasoconstriction was frequently observed in pulmonary arteries of B6.TgL but not in wild-type B6, BALB, and BALB.TgL mice, irrespective of the presence of the overt pathological changes mentioned above (data not shown). Perivascular lymphocytic infiltration was also observed around pulmonary veins; however, there was no pathologic remodeling in those veins as observed in the

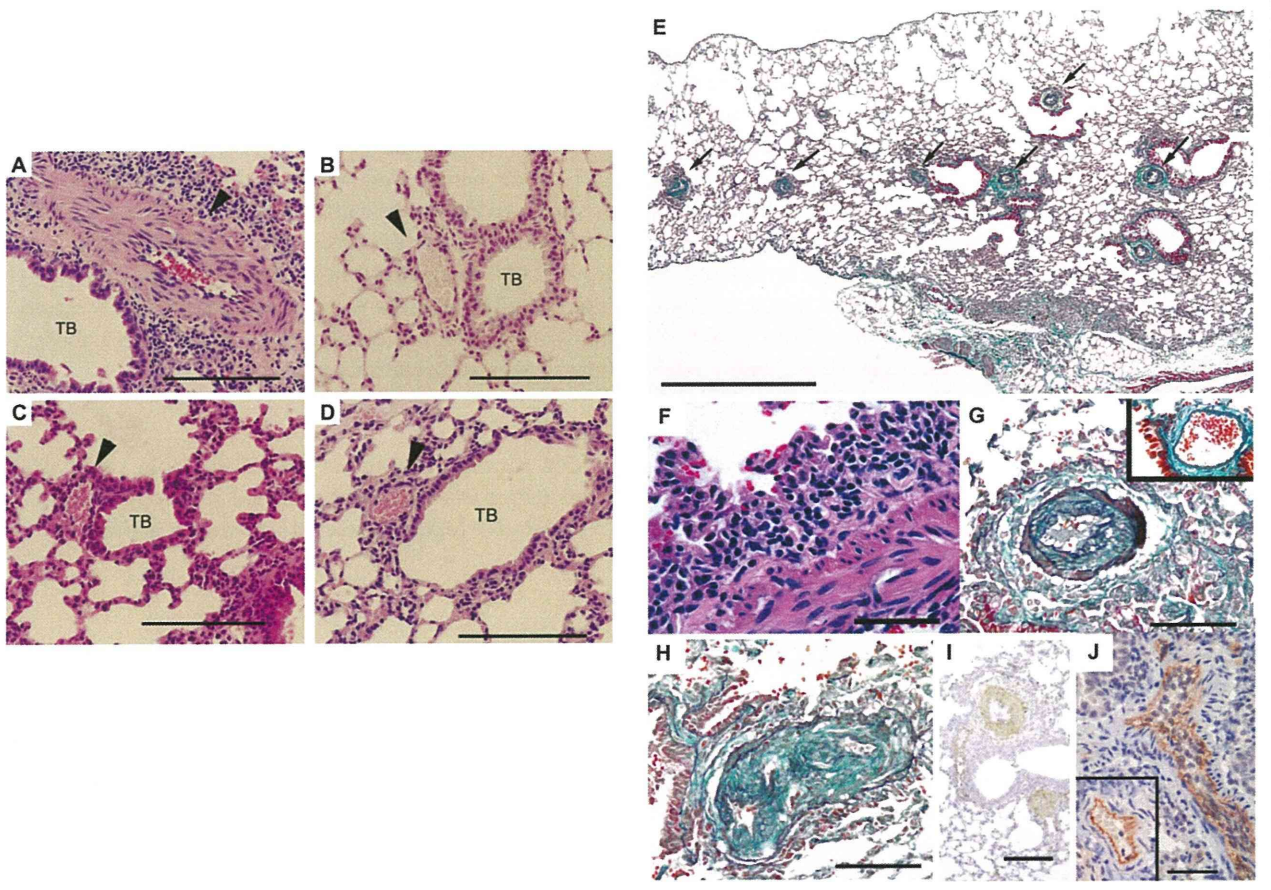

Figure 1 Histopathological features of the lung disease in B6.TgL mice. (A-D) Histopathological manifestation typically present in B6.TgL (A). No pathological manifestation observed in B6 (B), BALB.TgL (C), and BALB (D). The photograms indicated were taken from over 20-week aged male mouse. Arrow heads indicate pulmonary arteries. *TB*, terminal bronchiole. H&E staining. Scale bar = 100 μm. (E) Diffuse pathology present in B6.TgL. Masson's trichrome staining. Scale bar = 1 mm. (F) Perivascular lymphocytic infiltration in the affected lung. H&E staining. Scale bar = 50 μm. (G, H) Representative microscopic appearance in the affected arteries in the B6.TgL lung. An inset photogram in *G* represents the appearance of a normal pulmonary artery. Thickening of the intimal and, to a lesser extent, medial layers with marked intimal fibrosis is characteristic of the affected arteries. Masson's trichrome staining. Scale bar = 100 μm. *I* and *J*, expression of αSMA and CD31 (PECAM), respectively in the thickened arterial wall. The photogram in the inset of *J* represents a normal manifestation of unaffected artery. Immunohistochemical staining with hematoxylin counter-staining. Scale bar: in *I*, 200 μm; in *J*, 100 μm.

arteries (data not shown). Degenerative or granulomatous vascular lesions were not observed in conjunction with the perivascular infiltration, indicating that the vascular lesion of interest is not related to any type of vasculitis syndrome. We found no vascular lesions in the kidney or the colon of B6.TgL mice. Thus, the spontaneous lung disease in B6.TgL mice was characterized by lung-specific, pulmonary artery-restricted intimal thickening with lymphocytic (chronic) inflammation. These histopathological characteristics are similar yet distinct in a few points from those of human PAH.

Strain-restricted onset of the lung disease

The PAH-like disease, as defined in the B6.TgL mice, was quantified with a PAH score in other strains of mice, including B6, BALB, BALB.TgL, BALB × B6.TgL (BCF1.TgL), and (BALB × B6) F1 × B6.TgL (BCN2.TgL). It was observed that wild-type and different TgL strains, such as BALB.TgL and BCF1.TgL, barely developed the PAH-like disease (Table 1). On the other hand, BCN2.TgL developed a PAH-like disease with a broader distribution of the PAH score than B6.TgL. There were no sex-related differences in the PAH scores (Table 1). These findings indicate that development of the PAH-like disease depends on both the effects of TgL and on an undefined B6-specific genetic background.

Elevation of RV systolic pressure and RV hypertrophy in B6.TgL

The PAH-like arteriopathy in B6.TgL mice indicated the onset of clinical PH. We therefore measured right ventricular (RV) systolic pressure (RVSP) in aged B6.TgL, BALB.TgL, and their wild-type strains. RVSP was significantly increased in the B6.TgL mice, as compared to B6 (Figure 2A). Importantly, the RVSP values were significantly correlated with the PAH scores (Figure 2B). Furthermore, significant RV hypertrophy was demonstrated for B6.TgL, as compared to B6 mice (Figure 2C). Increases in RVSP and RV hypertrophy were not observed in the BALB.TgL mice, as compared to B6 mice (additional file 2). In other experiments performed using wild-type BALB mice (30 w), there has been no evidence for RV hypertension or RV hypertrophy in BALB strain: RVSP = 21.3 ±2.72 mmHg, RV/(LV + IVS) = 0.25 ±0.026.

Accumulation of effector/memory $CD4^+$ T cells in OX40L-Tg mice

Previous studies performed with B6.TgL mice have demonstrated a selective increase in the number of $CD44^{high}CD62L^{low}$ effector/memory $CD4^+$ T cells in lymphoid and nonlymphoid tissues [17,19]. We examined whether the tissue distribution of effector/memory $CD4^+$ T cells was altered by the genetic background before the disease onset. Flow cytometric analyses revealed a significant increase in the number of effector/memory $CD4^+$ T cells in both the spleen (Figure 3A and 3B) and lungs (Figure 3C and 3D) in every TgL mouse examined. Importantly, this increase was not observed in a strain-specific manner, indicating that the development of PAH is not simply explained by the increase of effector/memory $CD4^+$ T cells.

Strain-specific profile of cytokine production by the lung $CD4^+$ T cells

The functionality of resident $CD4^+$ T cells in the lungs of TgL mice was determined by testing their ability to produce cytokines in response to anti-CD3 or PMA/ionomycin stimulation, respectively. Augmented IL-13 production was observed in the TgL-derived T cells and interestingly, this augmentation was greater in B6.TgL than in BALB.TgL (Figure 4A). Furthermore, a larger number of IL-17-producing $CD4^+$ T cells were observed in B6.TgL mice than in BALB.TgL (Figure 4B). IL-4 and IL-5 were not detected in stimulated lung cells by any strains (data not shown). These results indicate that the function of tissue resident CD4 T cells can be modulated by the excessive OX40 signals on B6 genetic background before disease onset.

Over-expression of OX40L in B6 background alters the balance between lung resident effector/memory T cells and regulatory T cells

$CD4^+CD25^+Foxp3^+$ T cells, usually denoted as T_{reg} cells, are known to control inflammatory responses by suppressing the activities of $Foxp3^-$ effector T cells [24]. Several independent studies have demonstrated that lung resident T_{reg} cells suppress type 2 immune responses and, consequently, reduce pulmonary inflammation [25-27]. We analyzed the population size of T_{reg} cells, defined as $CD4^+Foxp3^+$, in the lung of non-transgenic and TgL strains. Flow cytometric analyses revealed that the frequency and absolute number of T_{reg} cells increased in TgL strains in advance of the disease onset as compared with those in nontransgenic strains (Figure 5A and 5B). It was particularly noted that the increase of T_{reg} was less in B6.TgL than in BALB.TgL, suggesting that B6-specific genetic factors counteract development of T_{reg} cells in TgL mice. We also examined the ratio of Foxp3- effector/memory CD4 T cells (additional file 3) to Foxp3+ T_{reg} before disease onset. The data shows an increased ratio of effector/memory T cells to T_{reg} cells in the B6.TgL lung compared to the BALB.TgL lung (Figure 5C). These findings also suggest an important role of T_{reg} in regulating inflammation associated with the pathogenesis of PAH-like disease in B6.TgL mice.

Identification of a susceptibility locus for PAH

TgL-dependent PH developed in a strain-specific manner, suggesting that the genetic background had an effect

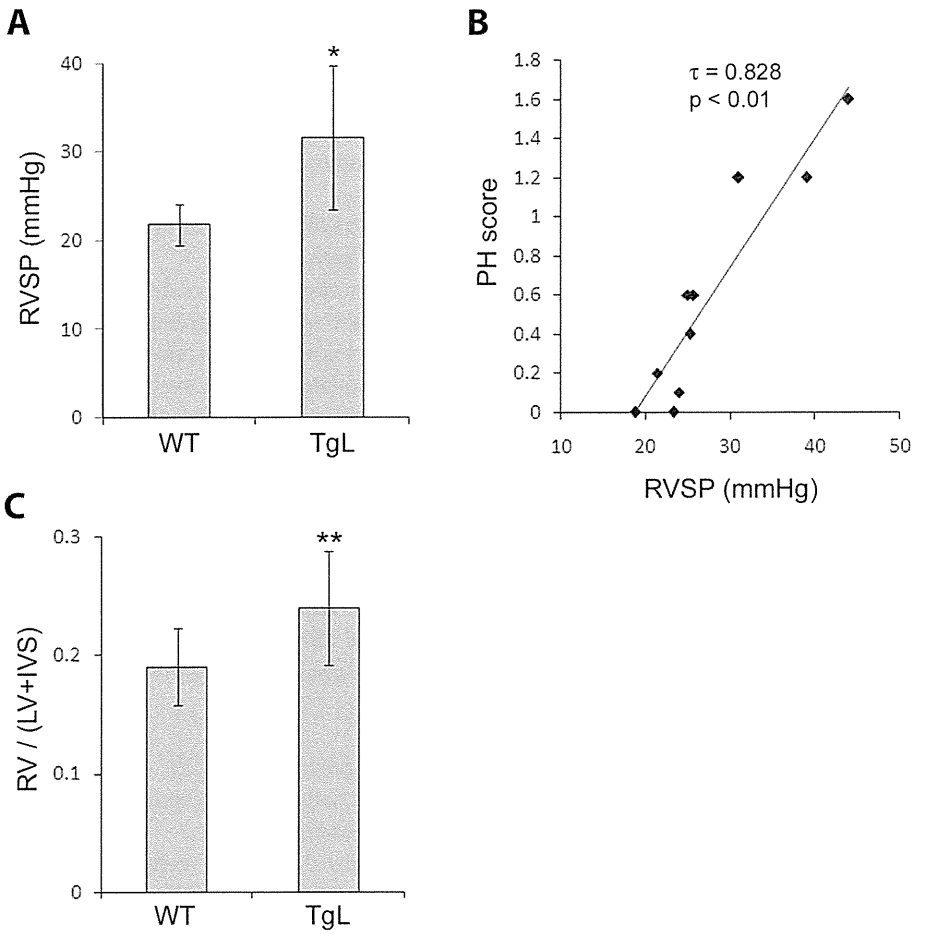

Figure 2 Clinicopathological phenotypes associated with PH. (A) Significant elevation of RVSP (mmHg) in B6.TgL. The result represents a mean ± standard deviation (SD) of 4 B6 or 6 B6.TgL mice (20 to 24 weeks old) for each group. (B) Correlation between RVSP values and PAH scores obtained from the 10 mice examined in *A*. The significance of this correlation was confirmed with the Kendall tau (τ) rank correlation coefficient (τ = 0.828). (C) RV hypertrophy manifested in B6.TgL. RV hypertrophy was evaluated with the index provided by the formula, RV/(LV+IVS). The result represents a mean ± SD of 12 B6 or 8 B6.TgL mice for each group. The significant difference between the two groups was evaluated by two-tailed *t*-test. *, $p < 0.05$; **, $p < 0.01$.

on the disease phenotypes. To identify a susceptibility locus for a PAH-like disease in B6.TgL, a genetic approach was employed using BCN2.TgL mice, which are descended from the B6.TgL and non-disease-prone BALB.TgL strains of mice. A genome-wide scan performed using selected 48 BCN2.TgL mice identified 4 candidate loci on chromosomes 5, 9, 13, and 17, which were possibly associated with the incidence of a PAH-like disease (additional file 1). The association study with 341 BCN2.TgL mice confirmed the suggestive association at *D5Mit346* (1 cM) and *D5Mit381* (8 cM) on chromosome 5 (Table 2). The other candidate loci preliminarily defined on chromosomes 9, 13, and 17 were not confirmed by this study. A QTL analysis consistently demonstrated a suggestive linkage between the level of PAH score and the chromosomal region between *D5Mit346* and *D5Mit381*. This linkage was observed in a single LOD peak of 2.4 at 7 cM on chromosome 5 (Figure 6).

Discussion

Previous studies have shown that B6.TgL mice display abnormal T-cell differentiation and functions, and spontaneous inflammation in the colon and lung. The colonic phenotype in B6.TgL mice was histopathologically defined as an inflammatory bowel disease resembling ulcerative colitis in humans. In the present study, the undetermined lung disease in B6.TgL mice was characterized as a PAH-like disease. PAH is a clinical category of PH that comprises many different disease entities. Pathological manifestations of the PAH-like disease in B6.TgL mice are not completely parallel to those of idiopathic PAH. The differences between idiopathic PAH

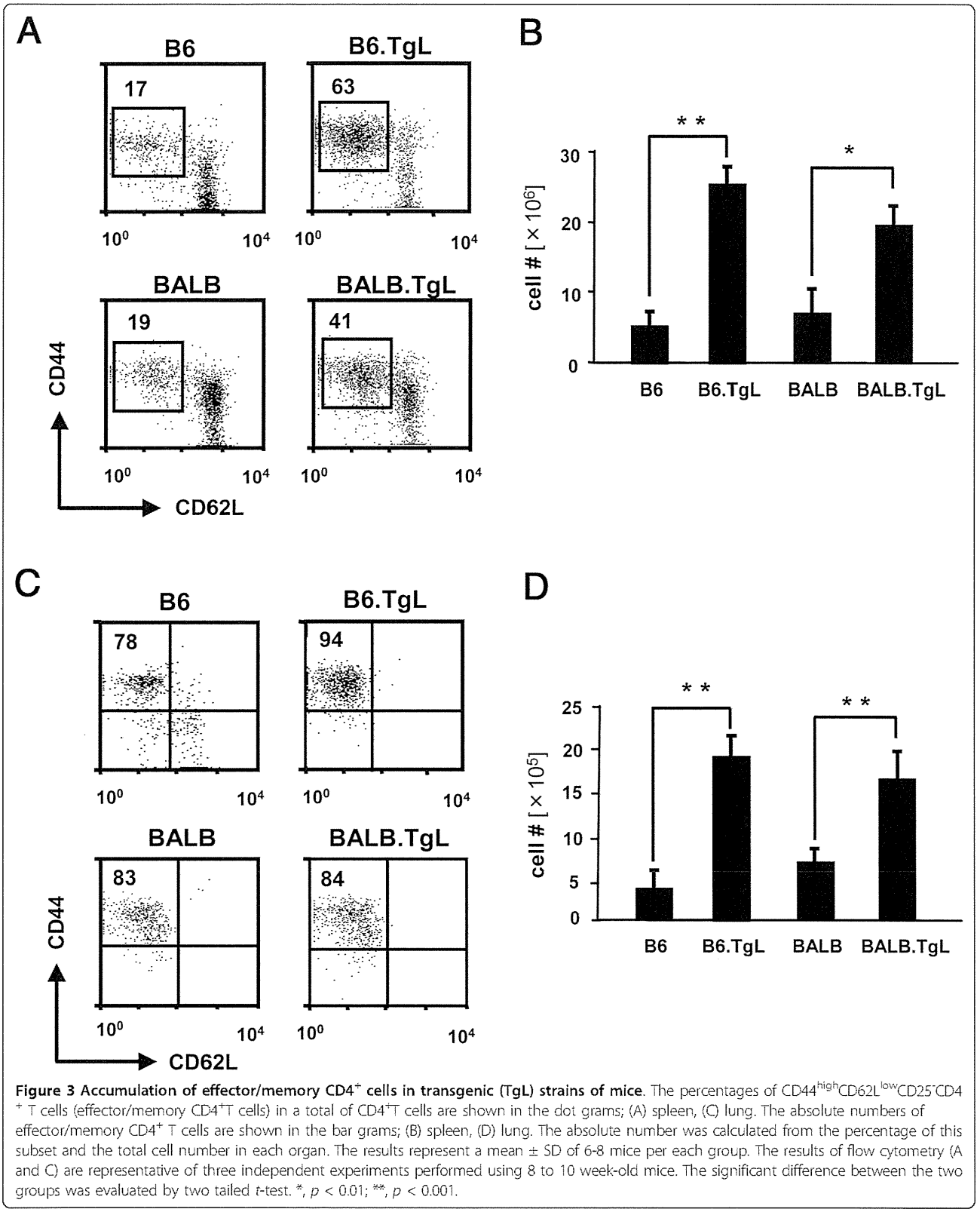

Figure 3 Accumulation of effector/memory CD4$^+$ cells in transgenic (TgL) strains of mice. The percentages of CD44^{high}CD62L^{low}CD25$^-$CD4$^+$ T cells (effector/memory CD4$^+$T cells) in a total of CD4$^+$T cells are shown in the dot grams; (A) spleen, (C) lung. The absolute numbers of effector/memory CD4$^+$ T cells are shown in the bar grams; (B) spleen, (D) lung. The absolute number was calculated from the percentage of this subset and the total cell number in each organ. The results represent a mean ± SD of 6-8 mice per each group. The results of flow cytometry (A and C) are representative of three independent experiments performed using 8 to 10 week-old mice. The significant difference between the two groups was evaluated by two tailed *t*-test. *, $p < 0.01$; **, $p < 0.001$.

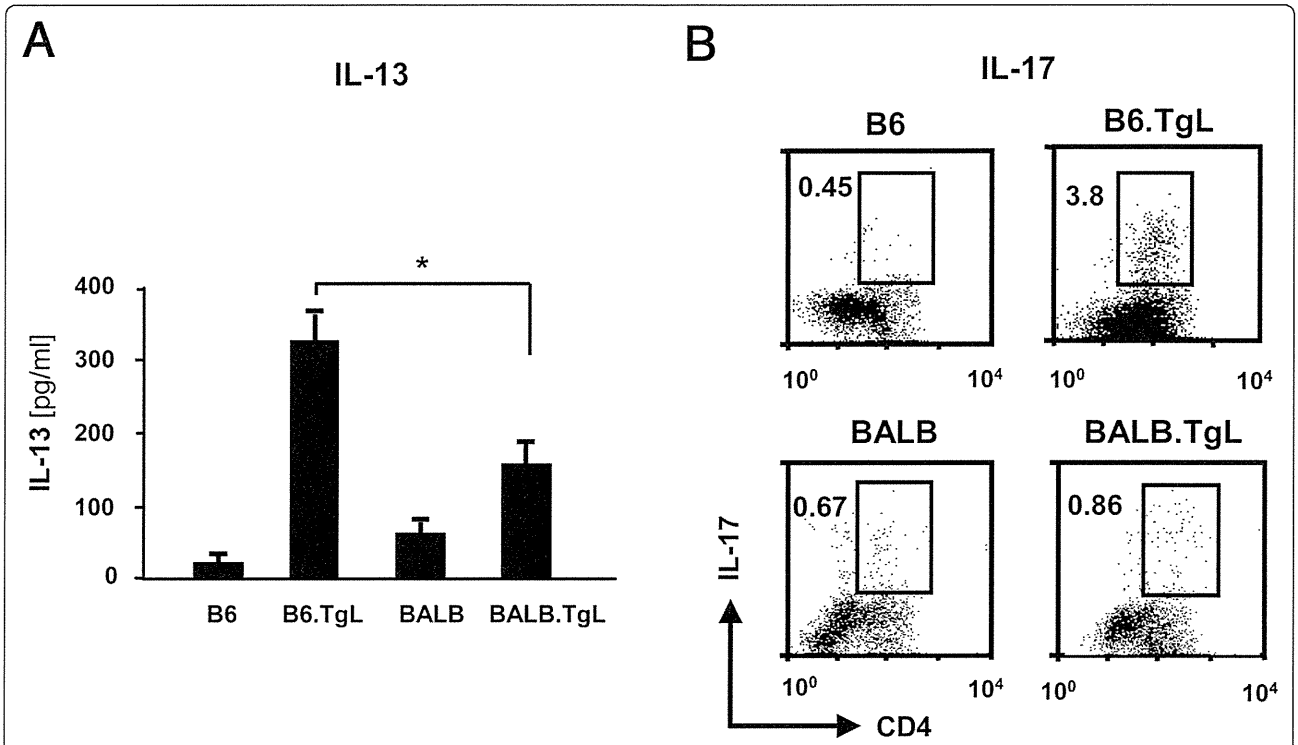

Figure 4 Strain-specific cytokine profile in lung CD4$^+$T cells. (A) IL-13 production from a total of lymphocytes isolated from the lung of non-transgenic and transgenic (TgL) strains of mice at 8 to 10 week-old. Lymphocytes containing equal number of CD44^{high}CD62L^{low}CD4$^+$T cells for each group (n = 4) of strain were stimulated with soluble anti-CD3 for 48 h and IL-13 in the cultured supernatant was quantified by ELISA. The significant difference between B6.TgL and BALB.TgL was evaluated by two-tailed *t*-test. *, $p < 0.05$. (B) IL-17 production in the lung CD4$^+$T cells. Lymphocytes isolated as above were incubated with PMA/Ionomycin in the presence of brefeldin A for 4 h and intracellular IL-17 production was analyzed in CD4 T cells. Representative data from two independent experiments were shown.

and the present animal model include the caliber of the affected arteries, the primarily affected layer of vascular wall, and the participation of massive lymphocytic perivascular infiltration. Further investigations are needed to define the present lung pathology as any type of PAH. An increasing body of evidence implicates the role of immune-mediated mechanisms in the pathogenesis of PAH. A type of PAH occurs secondarily to collagen vascular disorders, such as systemic sclerosis and mixed connective tissue disease (MCTD). Interestingly, PAH with MCTD presents with a prominent characteristic of endothelial degeneration and proliferation, probably due to the pathogenic contribution of autoantibodies to endothelial cells [28,29]. This characteristic may be a pathological consequence of immune-mediated mechanisms shared with the present model. The findings in the B6.TgL mice provide a possible insight into an implication of an OX40L-derived signal in the immune-mediated mechanism of endothelial pathology in PAH.

PAH is associated with endothelial cell dysfunction and vasoconstriction. There is no direct evidence for a link between these pulmonary vascular manifestations and abnormality *in situ* of OX40L-derived signal. However, it has been shown that OX40L-derived signals have a pathologic impact on the endothelial cell functions of systemic arteries. Recent studies have demonstrated an association of OX40L gene polymorphism with the susceptibility to atherosclerosis in humans [30], and the critical contribution of OX40-OX40L interactions to atherogenesis in low-density lipoprotein receptor-deficient mice [31]. The endothelial cells of the systemic arteries and those of the pulmonary arteries are exposed to different conditions, i.e., blood pressure and oxygen tension. It is interesting to know whether the OX40-OX40L interactions yield a different response on pulmonary endothelial cells than on systemic endothelial cells, and whether the OX40L gene polymorphism is associated with any type of PAH in humans.

Our present immunological studies performed using TgL and non-TgL strains of mice with different genetic backgrounds–B6 and BALB–revealed the respective effects of TgL and strain-dependent genetic background on immune phenotypes in the lung. Previous studies have demonstrated that OX40L-derived signals promote the expansion of effector/memory CD4$^+$ T cells [17,19]

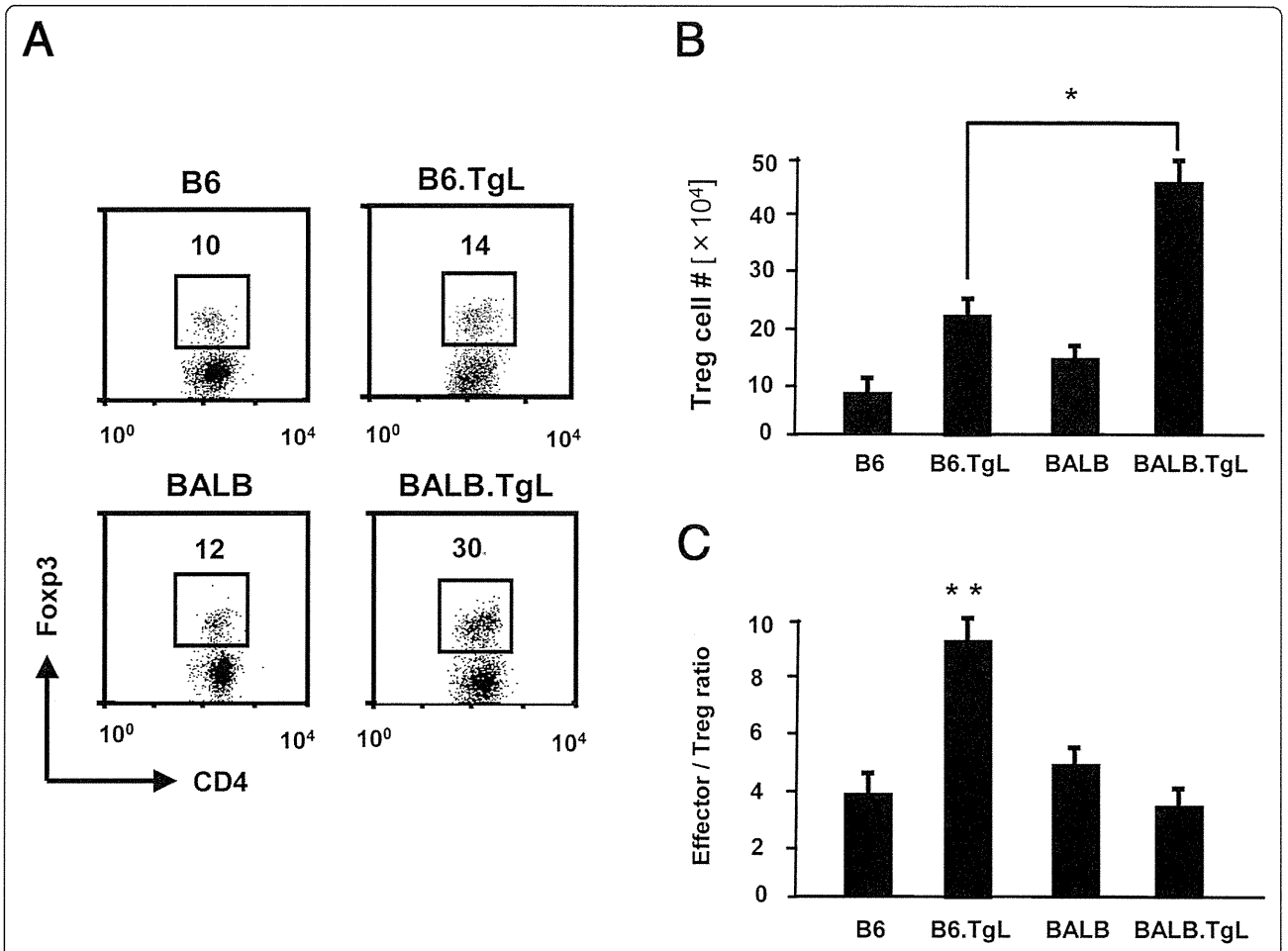

Figure 5 Accumulation of T_{reg} cells in non-transgenic and transgenic (TgL) strains of mice at 8 to 10 week-old. The percentage (A) and absolute numbers (B) of $CD4^+$ $Foxp3^+T_{reg}$ cells in the lung are shown. The absolute lymphocytic number was calculated from the percentage of T_{reg} and the total cell number. (C) The ratio of effector/memory T cells (CD4+ CD25- CD44 ^{high} CD62L ^{low}) to Fopx3+ T_{reg} cells in the lung. A significant increase in this ratio is shown in B6.TgL strain of mice. The result represents a mean ± SD from 4 mice per each group. The results of flow cytometry (A) are representative of two independent experiments. The significant difference between the two groups was evaluated by two tailed *t*-test. *, $p < 0.01$; **, $p < 0.001$.

and naturally arising T_{reg} cells [32], and enhance the production of IL-13 and IL-17 by $CD4^+$ T cells [33-35]. To examine which TgL-dependent immune aberrations are correlated with the onset of the PAH-like disease, we examined TgL-dependent immune phenotypes in the lungs of 2 different strains at a pre-disease stage. The findings indicate that B6-specific genetic factors influence the expansion of effector/memory $CD4^+$ T cells and T_{reg} cells in advance of the onset of lung disease. A possible role of T_{reg} cells has been documented in the

Table 2 Genetic association of PAH score in BCN2

Marker	Position (CM)	Mean of grade† BB	Mean of grade BC	P value‡
D5Mit346	1	0.51 ± 0.61 (172)	0.32 ± 0.46 (169)	0.0018 §
D5Mit381	8	0.51 ± 0.59 (178)	0.32 ± 0.46 (163)	0.0012 §
D5Mit197	36	0.46 ± 0.56 (192)	0.36 ± 0.52 (149)	0.0844
D5Mit338	59	0.45 ± 0.55 (191)	0.37 ± 0.53 (150)	0.1476
D5Mit213	70	0.41 ± 0.52 (192)	0.42 ± 0.58 (149)	0.9149
D5Mit409	83	0.42 ± 0.55 (165)	0.41 ± 0.54 (178)	0.766

* Values indicate mean ± SD and the values in parenthesis denote the number of mice.

† BB = B6 homozygote; BC = B6/BALB heterozygote

‡ The two-tail t-test. §, suggestive linkage [22].

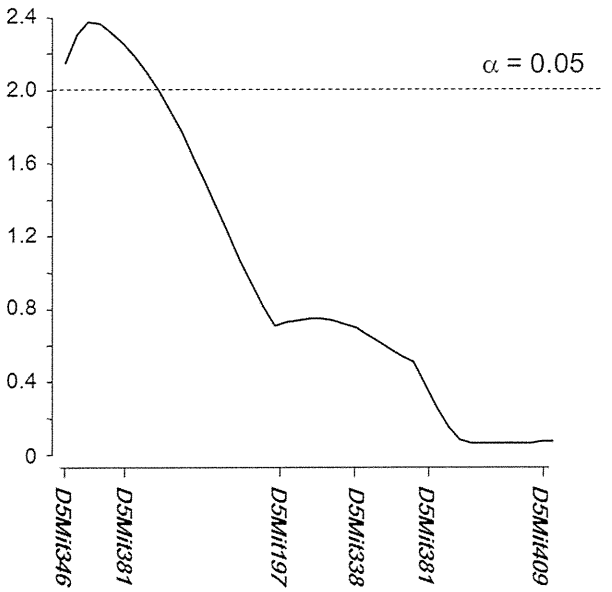

Figure 6 LOD plots of the QTL analysis for PAH scores on chromosome 5. The significant threshold level (α = 0.05) is shown by a score of 2 with a dashed line. The LOD peak (2.4) is located at 7 cM. The Y-axis denotes the level of the LOD score, and the X-axis denotes the genetic position defined by the microsatellite markers indicated: *D5Mit346* (1 cM), *D5Mit381* (8 cM), *D5Mit197* (36 cM), *D5Mit338* (59 cM), *D5Mit213* (70 cM), and *D5Mit409* (83 cM). The results were obtained using the interval mapping program of the MapMarker/QTL software.

development of PAH in humans [6]. Furthermore, it is clearly shown that B6-specific genetic factors increase the number of IL-17-producing $CD4^+$ T cells as well as secretion of IL-13 and IFNγ (data not shown) by lung tissue resident $CD4^+$ T cells. IL-17 producing CD4 T cells, namely Th17 cells are well known that participates in the pathogenesis of various organ-specific autoimmune diseases, such as inflammatory bowel disease and rheumatoid arthritis [36,37]. Although the role of Th17 cells in PAH in humans has not been determined, our present findings suggest that they indeed play a role in PAH. IL-13 serves as an important mediator in pulmonary inflammation [5,38,39], suggesting a causal contribution of IL-13 to the pathogenesis of the present model. The presence of immunological findings provides an insight into PAH-prone immune condition in the lung: the increase of proinflammatory effectors, IL-13 and Th17, and the decrease of an anti-inflammatory effector, T_{reg}.

The present genome-wide genetic approach demonstrated a new susceptibility locus controlling the onset of a PAH-like disease in our model. Previous genetic studies performed on familial PAH have shown mutations in 2 genes responsible for susceptibility to PAH: bone morphogenetic protein receptor 2 gene (*BMPR2*) [40] and activin-like kinase type-1 gene (*ALK-1*) [41]. Our identified locus includes neither of these genes, nor, to the best of our knowledge, any gene involved in their signal transduction pathways. However, *Nos3* and *Hgf* genes were particularly noted within this locus. Nitric oxide (NO) is known as a potent endothelial cell-derived vasodilator and an inhibitor of smooth muscle proliferation. Endothelial NO production largely depends on NOS3/eNOS (encoded by *Nos3*). NOS3-deficient mice showed reduced pulmonary vascular proliferation and remodeling to chronic hypoxia [42,43]. Several studies have reported the preventive role of NO in the development of PH in mice and humans. The polymorphism of human *Nos3* gene is associated with high-altitude pulmonary edema and PH in patients with chronic obstructive pulmonary disease [44]. On the other hand, *Hgf*, which encodes hepatocyte growth factor (HGF), suppresses vascular medial hyperplasia and matrix accumulation in advanced PH in rats [45]. These findings have underscored the role of NOS3/eNOS or HGF as a pathogenic modifier in the present PH model.

A T-cell subset, type II helper T cell (Th2), plays an important role in the pathogenesis of PAH in mice [39]. In this regard, it is noteworthy that the 2 loci (the transgene locus and the susceptibility locus) have a strong impact on Th1/Th2 balance. The OX40 signal promotes a Th2-prone condition in mice [34]. On the other hand, NO and HGF serve as inducible factors for type I helper T cells (Th1) [46,47]. Therefore, in the TgL strains of mice, the 2 loci are mutually counterbalanced, and the net Th1/Th2 proportion depends mainly on the polymorphic effect of the susceptibility locus. In a B6 genetic background, an effect of the susceptibility locus may suppress Th1 responses and maximize Th2 augmentation in the lung conferred by the OX40L transgene, resulting in the B6-specific onset of PH.

Conclusion

The present study reported a novel transgenic mouse model for PH. This model differs from previous PH models, which include a hypoxia-induced model, a drug-induced model, and a genetic model (i.e., endothelin B receptor-deficient) [48], in etiology, histopathology, and spontaneity of PH. Considering the physiological functions of OX40L, it is likely that the development of PH in the present model depends on Th2-mediated mechanisms. The present model may provide a new experimental opportunity for investigating immune-mediated mechanisms underlying PAH and the development of immune-targeted therapy for PAH.

Additional material

Additional file 1: Summary of genome wide scan. Genotypes of BCN2.TgL mice were determined by polymerase chain reaction (PCR) using genomic DNA for 98 microsatellite positions.

Additional file 2: Pathological phenotypes in the lung of BALB.TgL mice. (A) RVSP (mmHg) in BALB.TgL (35 w, male, n = 4) and wild-type B6 (28 w, male, n = 4). The difference in the average values between the two strains is not statistically significant (p = 0.37, two tailed t test). These RVSP values tended to be lower than those in our previous measurement shown in Figure 2A. This change is probably due to the difference in the experimental conditions. (B) Evaluation of RV hypertrophy in BALB.TgL (35 w, male, n = 5) and wild-type B6 (28 w, male, n = 5). RV hypertrophy was evaluated with the index of RV/(LV +IVS). The difference between the two strains is not statistically significant (p = 0.76, two-tailed t-test).

Additional file 3: Foxp3 expression on total CD4 versus CD25 negative effector CD4 T cells. Total CD4 and CD4+CD62L^{low}CD25 negative cells from the lung tissue were stained for intracellular Foxp3.

List of Abbreviations

αSMA: Alpha smooth muscle actin; B6.TgL: OX40L transgenic on C75BL/6 strain; BALB. TgL: OX40L transgenic on BALB/c strain; H & E: Hematoxylin and Eosin; HGF: Hepatocyte growth factor; IVS: Intraventricular Septum; LOD: Logarithm of odd; LV: Left ventricular; MCTD: Mixed connective tissue disease; NO: Nitric oxide; OX40L: OX40 ligand; PH: Pulmonary hypertension; PAH: Pulmonary arterial hypertension; PMA: phorbol 12-myristate 13-acetate; QTL: quantitative trait locus; RV: Right ventricle; RVSP: Right ventricular systolic pressure; Th: T helper cells; T reg: regulatory T cell; TNFSF: Tumor necrosis super-family

Acknowledgements

We would like to thank Drs. Mingcai Zhang, Hiroshi Furukawa, Hiroyuki Kumagai, Shigeki Shibahara, Yasushi Hoshikawa, and Masahisa Kyogoku for providing helpful, critical comments, Mr. Shin-ichi Tanaka and Miss Naomi Yamaki for technical help in the RVSP measurement, and Mrs. Emi Yura for secretarial help. This work was supported by grants: No.19390108 & No.19659096, Grants-in-Aid for Scientific Research from the Ministry of Education, Science, Sports, and Culture of Japan. CREST, JST.

Author details

[1]Department of Pathology, Tohoku University Graduate School of Medicine, 2-1 Seiryo, Aoba-ku, Sendai, Miyagi 980-8575 Japan. [2]Department of Immunology, Tohoku University Graduate School of Medicine, 2-1 Seiryo, Aoba-ku, Sendai, Miyagi 980-8575 Japan. [3]Department of Cardiovascular Medicine, Tohoku University Graduate School of Medicine, 2-1 Seiryo, Aoba-ku, Sendai, Miyagi 980-8575 Japan. [4]Department of Pharmacology and Medicine and Center for Lung Biology, University of South Alabama, College of Medicine, 307 University Blvd N Mobile, AL 36688-0002 USA. [5]Department of Pathology, Ehime University Graduate School of Medicine, Shitsukawa, Toon, Ehime 791-0295 Japan. [6]Japan Science and Technology Agency, CREST, Tokyo, Japan. [7]Johnson & Johnson Pharmaceutical Research & Development, L.L.C, 3210 Merryfield Row, San Diego, California 92121, USA.

Authors' contributions

MR and MO (Ono) conceived the project and contributed to all the aspect of this research. MN contributed to the genetic findings. MY, MO (Oka), and IFM contributed to histopathological findings. PS, NI, and KS (Sugamura) contributed to immunological findings. KS (Satoh) and HS contributed to physical findings such as blood pressure measurements. All authors read and approved the final manuscript.

Competing interests

The authors declare that they have no competing interests.

Received: 16 June 2011 Accepted: 15 December 2011
Published: 15 December 2011

References

1. Veeraraghavan S, Koss MN, Sharma OP: **Pulmonary veno-occlusive disease.** *Curr Opin Pulm Med* 1999, **5(5)**:310-313.
2. Dorfmuller P, Perros F, Balabanian K, Humbert M: **Inflammation in pulmonary arterial hypertension.** *Eur Respir J* 2003, **22(2)**:358-363.
3. Humbert M, Morrell NW, Archer SL, Stenmark KR, MacLean MR, Lang IM, Christman BW, Weir EK, Eickelberg O, Voelkel NF, *et al*: **Cellular and molecular pathobiology of pulmonary arterial hypertension.** *J Am Coll Cardiol* 2004, **43(12 Suppl S)**:13S-24S.
4. Golembeski SM, West J, Tada Y, Fagan KA: **Interleukin-6 causes mild pulmonary hypertension and augments hypoxia-induced pulmonary hypertension in mice.** *Chest* 2005, **128(6 Suppl)**:572S-573S.
5. Hoshino T, Kato S, Oka N, Imaoka H, Kinoshita T, Takei S, Kitasato Y, Kawayama T, Imaizumi T, Yamada K, *et al*: **Pulmonary Inflammation and Emphysema: Role of the Cytokines IL-18 and IL-13.** *Am J Respir Crit Care Med* 2007, **176(1)**:49-62.
6. Nicolls MR, Taraseviciene-Stewart L, Rai PR, Badesch DB, Voelkel NF: **Autoimmunity and pulmonary hypertension: a perspective.** *Eur Respir J* 2005, **26(6)**:1110-1118.
7. Taraseviciene-Stewart L, Nicolls MR, Kraskauskas D, Scerbavicius R, Burns N, Cool C, Wood K, Parr JE, Boackle SA, Voelkel NF: **Absence of T cells confers increased pulmonary arterial hypertension and vascular remodeling.** *Am J Respir Crit Care Med* 2007, **175(12)**:1280-1289.
8. Lenschow DJ, Walunas TL, Bluestone JA: **CD28/B7 system of T cell costimulation.** *Annu Rev Immunol* 1996, **14**:233-258.
9. Croft M: **Co-stimulatory members of the TNFR family: keys to effective T-cell immunity?** *Nat Rev Immunol* 2003, **3(8)**:609-620.
10. Sugamura K, Ishii N, Weinberg AD: **Therapeutic targeting of the effector T-cell co-stimulatory molecule OX40.** *Nat Rev Immunol* 2004, **4(6)**:420-431.
11. Mestas J, Crampton SP, Hori T, Hughes CC: **Endothelial cell co-stimulation through OX40 augments and prolongs T cell cytokine synthesis by stabilization of cytokine mRNA.** *Int Immunol* 2005, **17(6)**:737-747.
12. Kotani A, Hori T, Matsumura Y, Uchiyama T: **Signaling of gp34 (OX40 ligand) induces vascular endothelial cells to produce a CC chemokine RANTES/CCL5.** *Immunol Lett* 2002, **84(1)**:1-7.
13. Gramaglia I, Weinberg AD, Lemon M, Croft M: **Ox-40 ligand: a potent costimulatory molecule for sustaining primary CD4 T cell responses.** *J Immunol* 1998, **161(12)**:6510-6517.
14. Murata K, Ishii N, Takano H, Miura S, Ndhlovu LC, Nose M, Noda T, Sugamura K: **Impairment of antigen-presenting cell function in mice lacking expression of OX40 ligand.** *J Exp Med* 2000, **191(2)**:365-374.
15. Rogers PR, Song J, Gramaglia I, Killeen N, Croft M: **OX40 promotes Bcl-xL and Bcl-2 expression and is essential for long-term survival of CD4 T cells.** *Immunity* 2001, **15(3)**:445-455.
16. Soroosh P, Ine S, Sugamura K, Ishii N: **OX40-OX40 ligand interaction through T cell-T cell contact contributes to CD4 T cell longevity.** *J Immunol* 2006, **176(10)**:5975-5987.
17. Soroosh P, Ine S, Sugamura K, Ishii N: **Differential Requirements for OX40 Signals on Generation of Effector and Central Memory CD4+ T Cells.** *J Immunol* 2007, **179(8)**:5014-5023.
18. Maxwell JR, Weinberg A, Prell RA, Vella AT: **Danger and OX40 receptor signaling synergize to enhance memory T cell survival by inhibiting peripheral deletion.** *J Immunol* 2000, **164(1)**:107-112.
19. Murata K, Nose M, Ndhlovu LC, Sato T, Sugamura K, Ishii N: **Constitutive OX40/OX40 ligand interaction induces autoimmune-like diseases.** *J Immunol* 2002, **169(8)**:4628-4636.
20. Satoh K, Kagaya Y, Nakano M, Ito Y, Ohta J, Tada H, Karibe A, Minegishi N, Suzuki N, Yamamoto M, *et al*: **Important role of endogenous erythropoietin system in recruitment of endothelial progenitor cells in hypoxia-induced pulmonary hypertension in mice.** *Circulation* 2006, **113(11)**:1442-1450.
21. Marzo AL, Vezys V, Williams K, Tough DF, Lefrancois L: **Tissue-level regulation of Th1 and Th2 primary and memory CD4 T cells in response to Listeria infection.** *J Immunol* 2002, **168(9)**:4504-4510.
22. Lander E, Kruglyak L: **Genetic dissection of complex traits: guidelines for interpreting and reporting linkage results.** *Nat Genet* 1995, **11(3)**:241-247.
23. Morris JA, Gardner MJ: **Calculating confidence intervals for relative risks (odds ratios) and standardised ratios and rates.** *Br Med J (Clin Res Ed)* 1988, **296(6632)**:1313-1316.
24. Sakaguchi S: **Naturally arising CD4+ regulatory t cells for immunologic self-tolerance and negative control of immune responses.** *Annu Rev Immunol* 2004, **22**:531-562.
25. Hadeiba H, Locksley RM: **Lung CD25 CD4 regulatory T cells suppress type 2 immune responses but not bronchial hyperreactivity.** *J Immunol* 2003, **170(11)**:5502-5510.

26. Lewkowich IP, Herman NS, Schleifer KW, Dance MP, Chen BL, Dienger KM, Sproles AA, Shah JS, Kohl J, Belkaid Y, *et al*: **CD4+CD25+ T cells protect against experimentally induced asthma and alter pulmonary dendritic cell phenotype and function.** *J Exp Med* 2005, **202(11)**:1549-1561.
27. McKinley L, Logar AJ, McAllister F, Zheng M, Steele C, Kolls JK: **Regulatory T cells dampen pulmonary inflammation and lung injury in an animal model of pneumocystis pneumonia.** *J Immunol* 2006, **177(9)**:6215-6226.
28. Bodolay E, Csipo I, Gal I, Sipka S, Gyimesi E, Szekanecz Z, Szegedi G: **Anti-endothelial cell antibodies in mixed connective tissue disease: frequency and association with clinical symptoms.** *Clin Exp Rheumatol* 2004, **22(4)**:409-415.
29. Vegh J, Szodoray P, Kappelmayer J, Csipo I, Udvardy M, Lakos G, Aleksza M, Soltesz P, Szilagyi A, Zeher M, *et al*: **Clinical and immunoserological characteristics of mixed connective tissue disease associated with pulmonary arterial hypertension.** *Scand J Immunol* 2006, **64(1)**:69-76.
30. Wang X, Ria M, Kelmenson PM, Eriksson P, Higgins DC, Samnegard A, Petros C, Rollins J, Bennet AM, Wiman B, *et al*: **Positional identification of TNFSF4, encoding OX40 ligand, as a gene that influences atherosclerosis susceptibility.** *Nat Genet* 2005, **37(4)**:365-372.
31. van Wanrooij EJ, van Puijvelde GH, de Vos P, Yagita H, van Berkel TJ, Kuiper J: **Interruption of the Tnfrsf4/Tnfsf4 (OX40/OX40L) pathway attenuates atherogenesis in low-density lipoprotein receptor-deficient mice.** *Arterioscler Thromb Vasc Biol* 2007, **27(1)**:204-210.
32. Takeda I, Ine S, Killeen N, Ndhlovu LC, Murata K, Satomi S, Sugamura K, Ishii N: **Distinct roles for the OX40-OX40 ligand interaction in regulatory and nonregulatory T cells.** *J Immunol* 2004, **172(6)**:3580-3589.
33. Ohshima Y, Yang LP, Uchiyama T, Tanaka Y, Baum P, Sergerie M, Hermann P, Delespesse G: **OX40 costimulation enhances interleukin-4 (IL-4) expression at priming and promotes the differentiation of naive human CD4(+) T cells into high IL-4-producing effectors.** *Blood* 1998, **92(9)**:3338-3345.
34. Hoshino A, Tanaka Y, Akiba H, Asakura Y, Mita Y, Sakurai T, Takaoka A, Nakaike S, Ishii N, Sugamura K, *et al*: **Critical role for OX40 ligand in the development of pathogenic Th2 cells in a murine model of asthma.** *Eur J Immunol* 2003, **33(4)**:861-869.
35. Nakae S, Saijo S, Horai R, Sudo K, Mori S, Iwakura Y: **IL-17 production from activated T cells is required for the spontaneous development of destructive arthritis in mice deficient in IL-1 receptor antagonist.** *Proc Natl Acad Sci USA* 2003, **100(10)**:5986-5990.
36. Kotake S, Udagawa N, Takahashi N, Matsuzaki K, Itoh K, Ishiyama S, Saito S, Inoue K, Kamatani N, Gillespie MT, *et al*: **IL-17 in synovial fluids from patients with rheumatoid arthritis is a potent stimulator of osteoclastogenesis.** *J Clin Invest* 1999, **103(9)**:1345-1352.
37. Fujino S, Andoh A, Bamba S, Ogawa A, Hata K, Araki Y, Bamba T, Fujiyama Y: **Increased expression of interleukin 17 in inflammatory bowel disease.** *Gut* 2003, **52(1)**:65-70.
38. Zhu Z, Ma B, Zheng T, Homer RJ, Lee CG, Charo IF, Noble P, Elias JA: **IL-13-induced chemokine responses in the lung: role of CCR2 in the pathogenesis of IL-13-induced inflammation and remodeling.** *J Immunol* 2002, **168(6)**:2953-2962.
39. Daley E, Emson C, Guignabert C, de Waal Malefyt R, Louten J, Kurup VP, Hogaboam C, Taraseviciene-Stewart L, Voelkel NF, Rabinovitch M, *et al*: **Pulmonary arterial remodeling induced by a Th2 immune response.** *J Exp Med* 2008, **205(2)**:361-372.
40. Deng Z, Morse JH, Slager SL, Cuervo N, Moore KJ, Venetos G, Kalachikov S, Cayanis E, Fischer SG, Barst RJ, *et al*: **Familial primary pulmonary hypertension (gene PPH1) is caused by mutations in the bone morphogenetic protein receptor-II gene.** *Am J Hum Genet* 2000, **67(3)**:737-744.
41. Morse JH, Deng Z, Knowles JA: **Genetic aspects of pulmonary arterial hypertension.** *Ann Med* 2001, **33(9)**:596-603.
42. Quinlan TR, Li D, Laubach VE, Shesely EG, Zhou N, Johns RA: **eNOS-deficient mice show reduced pulmonary vascular proliferation and remodeling to chronic hypoxia.** *Am J Physiol Lung Cell Mol Physiol* 2000, **279(4)**:L641-650.
43. Steudel W, Scherrer-Crosbie M, Bloch KD, Weimann J, Huang PL, Jones RC, Picard MH, Zapol WM: **Sustained pulmonary hypertension and right ventricular hypertrophy after chronic hypoxia in mice with congenital deficiency of nitric oxide synthase 3.** *J Clin Invest* 1998, **101(11)**:2468-2477.
44. Droma Y, Hanaoka M, Ota M, Katsuyama Y, Koizumi T, Fujimoto K, Kobayashi T, Kubo K: **Positive association of the endothelial nitric oxide synthase gene polymorphisms with high-altitude pulmonary edema.** *Circulation* 2002, **106(7)**:826-830.
45. Ono M, Sawa Y, Mizuno S, Fukushima N, Ichikawa H, Bessho K, Nakamura T, Matsuda H: **Hepatocyte growth factor suppresses vascular medial hyperplasia and matrix accumulation in advanced pulmonary hypertension of rats.** *Circulation* 2004, **110(18)**:2896-2902.
46. Ito W, Kanehiro A, Matsumoto K, Hirano A, Ono K, Maruyama H, Kataoka M, Nakamura T, Gelfand EW, Tanimoto M: **Hepatocyte growth factor attenuates airway hyperresponsiveness, inflammation, and remodeling.** *Am J Respir Cell Mol Biol* 2005, **32(4)**:268-280.
47. Niedbala W, Wei XQ, Campbell C, Thomson D, Komai-Koma M, Liew FY: **Nitric oxide preferentially induces type 1 T cell differentiation by selectively up-regulating IL-12 receptor beta 2 expression via cGMP.** *Proc Natl Acad Sci USA* 2002, **99(25)**:16186-16191.
48. Ivy DD, McMurtry IF, Colvin K, Imamura M, Oka M, Lee DS, Gebb S, Jones PL: **Development of occlusive neointimal lesions in distal pulmonary arteries of endothelin B receptor-deficient rats: a new model of severe pulmonary arterial hypertension.** *Circulation* 2005, **111(22)**:2988-2996.

doi:10.1186/1471-2172-12-67
Cite this article as: Rabieyousefi *et al.*: Indispensable roles of OX40L-derived signal and epistatic genetic effect in immune-mediated pathogenesis of spontaneous pulmonary hypertension. *BMC Immunology* 2011 12:67.

blood

2010 116: 1971-1979
Prepublished online June 10, 2010;
doi:10.1182/blood-2010-02-269134

PKCζ decreases eNOS protein stability via inhibitory phosphorylation of ERK5

Patrizia Nigro, Jun-ichi Abe, Chang-Hoon Woo, Kimio Satoh, Carolyn McClain, Michael R. O'Dell, Hakjoo Lee, Jae-Hyang Lim, Jian-dong Li, Kyung-Sun Heo, Keigi Fujiwara and Bradford C. Berk

Blood (print ISSN 0006-4971, online ISSN 1528-0020), is published weekly by the American Society of Hematology, 2021 L St, NW, Suite 900, Washington DC 20036.

PKCζ decreases eNOS protein stability via inhibitory phosphorylation of ERK5

Patrizia Nigro,[1] Jun-ichi Abe,[1] Chang-Hoon Woo,[2] Kimio Satoh,[3] Carolyn McClain,[1] Michael R. O'Dell,[1] Hakjoo Lee,[1] Jae-Hyang Lim,[4] Jian-dong Li,[4] Kyung-Sun Heo,[1] Keigi Fujiwara,[1] and Bradford C. Berk[1]

[1]Aab Cardiovascular Research Institute and Department of Medicine, University of Rochester Medical Center, NY; [2]Department of Pharmacology, College of Medicine, Yeungnam University, Daegu, Korea; [3]Department of Cardiovascular Medicine, Tohoku University Graduate School of Medicine, Sendai, Japan; and [4]Department of Microbiology and Immunology, University of Rochester Medical Center, NY

PKCζ has emerged as a pathologic mediator of endothelial cell dysfunction, based on its essential role in tumor necrosis factor α (TNFα)–mediated inflammation. In contrast, extracellular signal–regulated kinase 5 (ERK5) function is required for endothelial cell homeostasis as shown by activation of Krüppel-like factor 2 (KLF2), increased endothelial nitric-oxide synthase (eNOS) expression, and inhibition of apoptosis. We hypothesized that protein kinase C ζ (PKCζ) activation by TNFα would inhibit the ERK5/KLF2/eNOS pathway. TNFα inhibited the steady laminar flow–induced eNOS expression, and this effect was reversed by the dominant-negative form of PKCζ (Ad.DN-PKCζ). In addition, ERK5 function was inhibited by either TNFα or the transfection of the catalytic domain of PKCζ. This inhibition was reversed by PKCζ small interfering RNA. PKCζ was found to bind to ERK5 under basal conditions with co-immunoprecipitation and the mammalian 2-hybrid assay. Furthermore, PKCζ phosphorylates ERK5, and mutation analysis showed that the preferred site is S486. Most importantly, we found that the predominant effect of TNFα stimulation of PKCζ was to decrease eNOS protein stability that was recapitulated by transfecting Ad.ERK5S486A mutant. Finally, aortic en face analysis of ERK5/PKCζ activity showed high PKCζ and ERK5 staining in the athero-prone region. Taken together our results show that PKCζ binds and phosphorylates ERK5, thereby decreasing eNOS protein stability and contributing to early events of atherosclerosis. (*Blood*. 2010;116(11): 1971-1979)

Introduction

Endothelial nitric-oxide synthase (eNOS) is a key enzyme involved in the regulation of vascular function, and the altered activity and expression of this enzyme has been shown to contribute to atherosclerosis.[1-4] It has been reported that eNOS is regulated at the transcriptional, posttranscriptional, and posttranslational levels.[5,6] For example, tumor necrosis factor α (TNFα) has been shown to inhibit eNOS expression by down-regulating both transcriptional and posttranscriptional processes.[7-9]

Inflammation plays a central role in the pathogenesis of atherosclerosis.[10-13] TNFα, in addition to regulating eNOS expression, is a mediator of inflammation, and protein kinase C ζ (PKCζ) is a key enzyme for the TNFα-mediated inflammation. When endothelial cells (ECs) are stimulated by TNFα, PKCζ is activated and promotes monocyte adhesion by increased nuclear factor-κB–dependent intercellular adhesion molecule 1 expression.[14,15] In addition, we found that PKCζ activity was required for TNFα-mediated activation of c-Jun N-terminal kinase and caspase-3 in ECs,[16] events that cause endothelial dysfunction. Interestingly, increased PKCζ phosphorylation (ie, active form of the enzyme) was found in ECs located in the athero-susceptible region of porcine aorta.[17] Together, these observations suggest an important role of PKCζ in the process of atherogenesis by up-regulating inflammatory pathways in ECs.

A distinctive characteristic of PKCζ is the presence at the N-terminus of a novel protein-protein interaction module, termed PB1. The PB1 domain is named after the prototypical domain found in Phox and Bem1p, which mediate polar-heterodimeric interactions.[18] This domain is also present in the mitogen extracellular-signal-regulated kinase kinase 5 (MEK5), the upstream activator of the extracellular signal-regulated kinase 5 (ERK5), suggesting that there may be a cross talk between the PKCζ atherogenic and the MEK5-ERK5-KLF2 (Krüppel-like factor 2) atheroprotective signaling pathways. This latter pathway is activated by steady laminar flow (s-flow) and inhibits atherosclerosis.[19,20]

The atheroprotective effects of s-flow are well known. For example, we have earlier reported that s-flow potently activates ERK5[21] and that this s-flow–mediated ERK5 activation induces the expression of KLF2, a recently identified transcriptional activator of eNOS and an inhibitor of EC inflammation.[22,23] Furthermore, we have shown that peroxisome proliferator activated receptor γ1 is activated by s-flow by way of ERK5 activation and contributes to the overall anti-inflammatory and athero-protective effects of flow.[24] In addition to its kinase activity, ERK5 acts as a transcriptional activator. The C-terminus region of ERK5 has 2 transactivation domains, one of them (aa684-806) is constitutively active. Importantly, proatherogenic stimuli inhibit ERK5 activity, in part by stimulating SUMOylation at Lys6 and Lys22, which decreases flow-mediated KLF2 promoter activity and eNOS expression.[25]

The mechanism by which TNFα decreases eNOS expression in ECs is not fully elucidated. Here, we study the involvement of PKCζ and the MEK5/ERK5 pathway in the TNFα-induced down-regulation of eNOS expression in ECs and in the initiation of atherosclerosis.

Submitted February 8, 2010; accepted May 23, 2010. Prepublished online as *Blood* First Edition paper, June 10, 2010; DOI 10.1182/blood-2010-02-269134.

The online version of this article contains a data supplement.

The publication costs of this article were defrayed in part by page charge payment. Therefore, and solely to indicate this fact, this article is hereby marked "advertisement" in accordance with 18 USC section 1734.

Methods

Antibodies, small interfering RNA, adenovirus, and reagents

Antibodies against ERK5 and p-PKCζ were purchased from Cell Signaling; anti-Flag and anti-tubulin from Sigma-Aldrich; anti-PKCζ, anti–hemagglutinin A (HA) and, anti–VP-16 from Santa Cruz Biotechnology Inc (CA); and anti-eNOS and anti– platelet endothelial cell adhesion molecule 1 (PECAM-1) from BD Transduction Laboratories. Peroxidase-conjugated goat anti–mouse and anti–rabbit antibodies were obtained from GE Healthcare. Alexa Fluor 488– or 546–conjugated goat anti–rabbit and anti–rat antibodies were purchased from Molecular Probes. The predesigned and prevalidated human-specific PKCζ small interfering RNA (siRNA; ON-TARGET plus SMART pool PKCζ siRNA; L-003526-00-00) and control siRNA were from Dharmacon RNA Technologies. Adenovirus that drives expression of a dominant-negative form of PKCζ (Ad.PKCζ-DN, ADV-112) was purchased from Cell Biolabs. TNFα was purchased from Roche Applied Science, and active recombinant human PKCζ was obtained from Stressgen Biotechnologies.

Plasmid construction

Mouse ERK5 and the constitutively active form of MEK5α (CA-MEK5α) were cloned as described previously.[26] PKCζ wild-type (WT) and catalytic domain (CATζ) constructs were kind gifts from Dr Jae-Won Soh (Columbia University), and eNOS promoter was a gift from Dr David Gardner (University of California, San Francisco). The reporter gene encoding KLF2 promoter (−924 to +14) was a gift from Dr Jerry Lingrel (University of Cincinnati). Gal4-ERK5 and VP16-ERK5 were created by inserting the mouse ERK5 isolated from pcDNA3.1-ERK5 into *Bam*H1 and *Not*1 sites of the pBIND and pACT vectors, respectively. Single mutations of ERK5 were created with the QuikChange site-directed mutagenesis kit (Stratagene). All constructs were verified by DNA sequencing.

Cell culture and transfection

Human umbilical vein endothelial cells (HUVECs) were obtained from collagenase-digested umbilical veins and collected in M200 medium supplemented with low serum growth supplement (Cascade Biologic), 5% fetal calf serum (GIBCO), 50 U/mL penicillin, and 50 μg/mL streptomycin. Bovine aortic ECs (BAECs) were cultured in M199 medium (GIBCO) supplemented with 10% fetal clone III (Hyclone), minimal essential medium (MEM)–amino acids, 50 U/mL penicillin, and 50 μg/mL streptomycin. HUVECs as well as BAECs were cultured on 2% gelatin precoated dishes. Chinese hamster ovary cells were cultured in F12 medium (GIBCO) supplemented with 10% fetal calf serum (GIBCO), 50 U/mL penicillin, and 50 μg/mL streptomycin. For transient expression experiments, 80% confluent cells were transfected with Opti-MEM and Lipofectamine 2000 (Invitrogen) as previously described.[27] Three hours after transfection, Opti-MEM was replaced with complete media, and cells were treated with TNFα 6 hours later.

For siRNA-driven depletion of PKCζ, HUVECs were transiently transfected with 40nM PKCζ or control siRNA with the use of Lipofectamine 2000 reagent. The cells were harvested 36 hours after siRNA transfection. For adenoviral infection, HUVECs were transduced with 50 multiplicity of infection of adenovirus expressing a dominant-negative form of PKCζ (Ad.PKCζ-DN)[28] and used 16 hours later.

Mammalian 1- or 2-hybrid analysis and transfection of cells

HUVECs were plated in 12-well plates at 5×10^4 cells/well. For mammalian one-hybrid analysis of transcriptional activity, cells were transfected in Opti-MEM with a Lipofectamine 2000 mixture containing pG5-luc vector, pBIND-ERK5, and pcDNA3 with or without pcDNA3-CA-MEKα. After 3 hours, cells were washed, and fresh medium supplemented with 10% fetal calf serum was added. Cells were treated 8 hours after transfection. For the mammalian 2-hybrid assay, cells were transfected in Opti-MEM with a Lipofectamine mixture containing the pG5-luc vector and various pBIND and pACT plasmids (Promega). Three hours later, Opti-MEM was replaced with complete medium, and cells were incubated overnight, washed twice with phosphate-buffered saline, and lysed in Passive Lysis Buffer (E194A; Promega). Luciferase assays were done with the Luciferase Assay system (E1501; Promega). Luciferase activity was normalized to β-galactosidase activity to correct for differences in transfection efficiency.

eNOS and KLF2 promoter activity

HUVECs were transiently cotransfected with human eNOS promoter (−1197) or KLF2 promoter (−924 to +14) and β-galactosidase with the use of Lipofectamine 2000. Luciferase activity was measured as above.

Steady laminar flow protocol

Confluent cells cultured in 100-mm dishes were exposed to s-flow (shear stress = 12 dyn/cm^2) with the use of a cone and plate type of flow apparatus placed in a humidified 5% CO_2 incubator at 37°C for 24 hours.

Western blot analysis and immunoprecipitation

Cells were harvested and lysed in RIPA buffer (5mM/L HEPES [N-2-hydroxyethylpiperazine;N′-2-ethanesulfonic acid], 10mM/L EDTA [ethylenediaminetetraacetic acid], 150mM/L NaCl, 1% NP-40, 0.5% sodium deoxycholate, 0.1% sodium dodecyl sulfate [SDS], pH 7.4) supplemented with the protease inhibitor cocktail.[29] Protein concentration was determined by Bradford assay (Bio-Rad), and cell lysates were subjected to SDS–polyacrylamide gel electrophoresis (PAGE). Proteins were then transferred onto nitrocellulose membranes, and the membranes were subsequently blocked with 5% nonfat dry milk in phosphate-buffered saline (PBS)/0.1% Tween20 for 1 hour. After being washed 3 times with PBS/0.1% Tween20, the blots were incubated overnight at 4°C with appropriate primary antibodies. Then, the membranes were incubated with peroxidase-conjugated secondary antibodies for 1 hour. Signals were visualized with the use of the enhanced chemiluminescence Western blotting detection system (Amersham Biosciences). Images were acquired with a Gel Doc System (Gel Doc 2000; Bio-Rad), and a densitometric analysis of membranes was performed using the Bio-Rad software. For the immunoprecipitation analysis, clarified supernatants (400 μg of total protein) were incubated with anti-Flag or anti-ERK5 at 4°C overnight. Lysates were then mixed with 50 μL of protein A/G agarose beads and incubated for 2 hours at 4°C. Immune complexes were collected by centrifugation (3000*g* for 2 minutes) and washed 4 times with the RIPA buffer, and then bound proteins were released in 2× SDS gel sample buffer. Then, the immunoprecipitates were subjected to SDS-PAGE and Western blot analysis.

In vitro phosphorylation of ERK5 by activated PKCζ

Glutathione-*S*-transferase (GST)–ERK5–truncated mutant proteins were expressed in *Escherichia coli*, purified with glutathione-Sepharose 4B as described (Pharmacia Biotech Inc), and used in in vitro kinase assays by activated PKCζ as described previously.[26] Briefly, each GST-ERK5 fragment (3 μg) was incubated for 30 minutes at 30°C in a reaction mixture (40 μL) containing 15 μmol/L adenosine triphosphate (ATP), 10mmol/L $MgCl_2$, 10mmol/L $MnCl_2$, 3 μCi (0.111 Bq) of [γ-^{32}P]ATP, and 10 ng of active recombinant human PKCζ. The reaction was terminated by adding 6 μL of 6× electrophoresis sample buffer and boiling for 5 minutes. Samples were analyzed on 10% SDS-PAGE, followed by autoradiography.

Real-time quantitative polymerase chain reaction analysis of eNOS and KLF2

Total RNA was isolated with the use of the TRIazol reagent (Invitrogen) and reverse transcription was conducted with the use of TaqMan reverse transcription reagents (Applied Biosystem) following the manufacturer's instruction. The relative quantities of specific mRNAs were obtained with the use of the comparative Ct method and were normalized to glyceraldehyde-3-phosphate dehydrogenase (Applied Biosystem).

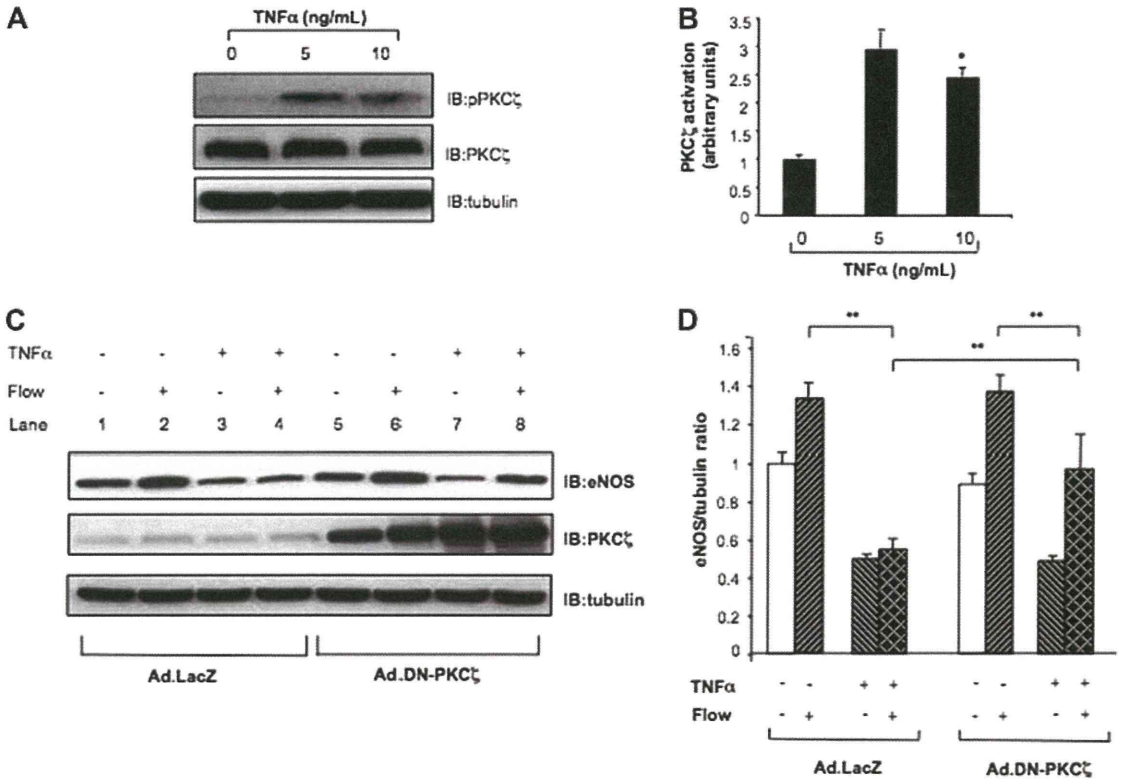

Figure 1. Reducing PKCζ activity by Ad.DN-PKCζ reverses TNFα inhibition of eNOS. (A-B) TNFα increases PKCζ activation/phosphorylation. (A) Confluent BAECs were exposed to TNFα 5 and 10 ng/mL or vehicle alone for 15 minutes. Then, cells were lysed and immunoblotted with p-PKCζ and total PKCζ antibodies, respectively. The amount of proteins loaded in each lane was equal as shown by incubating the same blots with antitubulin antibody. (B) Densitometric analysis of p-PKCζ. Results were normalized by arbitrarily setting the average densitometry of the control to 1.0. Representative blots are shown from 3 separate experiments. $^{*}P < .01$. (C-D) TNFα-mediated eNOS reduction is PKCζ dependent. (C) HUVECs were transfected with Ad.LacZ (control) or Ad.DN-PKCζ. After 16 hours cells were treated with TNFα or vehicle and then exposed to flow (shear stress = 12 dyn/cm^2) for 24 hours. Western blots were performed for eNOS, PKCζ, and tubulin. (D) eNOS expression was analyzed by densitometry and normalized by setting static cells to 1.0. Data are mean ± SD of 3 experiments in triplicate. $^{**}P < .05$.

Animal model and en face confocal analysis

All animal experiments were conducted in accordance with experimental protocols that were approved by the Institutional Animal Care and Use Committee at the University of Rochester. ApoE$^{-/-}$ mice on a C57BL/6J background were obtained from The Jackson Laboratory.

Immunofluorescence staining of mouse aortic ECs was performed as described previously.[30] Aortas of 12-week-old female ApoE$^{-/-}$ mice were perfused with PBS followed by 2% paraformaldehyde in PBS for 10 minutes. After fixation, the aortas were cut into small fragments and incubated in blocking buffer containing 2% bovine serum albumin and 0.1% Triton X-100 in PBS. Primary antibody incubations were performed overnight at 4°C. After washing the aortic segments 3 times, the secondary antibodies were added and incubated for 1 hour. For negative controls, nonimmune goat or rabbit immunoglobulin G was used in place of primary antibodies. After 3 washes, aortic specimens were opened, placed on a glass slide with the luminal side up, and then mounted for confocal microscopy (Olympus; FLUOVIEW300).

Statistical analysis

Data are shown as mean plus or minus SD for 3 to 4 separate experiments. Differences were analyzed by 1-way analysis of variance or Student *t* test. *P* values are expressed as less than .1 and less than .05. The latter was considered statistically significant.

Results

TNFα inhibits eNOS expression by a PKCζ-dependent pathway

To investigate the involvement of PKCζ activation in the TNFα-mediated inhibition of eNOS, we first treated BAECs with TNFα (0-10 ng/mL; 15 minutes), and PKCζ activity was measured by phosphorylation at Thr410 (p-PKCζ) by immunoblotting (Figure 1A-B). There was a significant 3-fold increase in PKCζ activity that was maximal at 5 ng/mL. TNFα treatment did not affect PKCζ expression in these cells (Figure 1A).

To study the effect of PKCζ activation on eNOS protein expression we used s-flow (12 dynes/cm^2; 24 hours) to stimulate eNOS expression. As shown in Figure 1C and D, s-flow increased eNOS expression by 1.3- plus or minus 0.09-fold ($N = 3$; $P < .05$). The addition of TNFα (10 ng/mL; 24 hours) had 2 significant effects on eNOS expression. First, there was a 55% decrease in expression (Figure 1D bars 1 vs 3), and second, the s-flow–mediated increase in eNOS expression (lanes 2 vs 1) was significantly inhibited by TNFα (lanes 4 vs 2). To determine whether this effect could be reversed by inhibiting PKCζ activity, we used the dominant-negative form of PKCζ (ATP binding site K to M mutant; DN-PKCζ). HUVECs were transduced with Ad.DN-PKCζ or adenoviral β-galactosidase (Ad.LacZ) and exposed to s-flow with or without TNFα. HUVECs transduced with Ad.LacZ expressed the same level of eNOS as sham-transfected cells (not shown) and Ad.DN-PKCζ (lanes 5 vs 1). Cells expressing Ad.DN-PKCζ exhibited an s-flow–mediated increase in eNOS expression (1.3-fold ± 0.1-fold; $N = 3$; $P < .05$) that did not differ from control Ad.LacZ-expressing cells (Figure 1C-D lanes 6 vs 2). More importantly, Ad.DN-PKCζ transduction significantly reduced the TNFα-mediated inhibition of eNOS expression in HUVECs exposed to s-flow (43% increase; Figure 1C lanes 8 vs 4). These data show that eNOS expression induced by s-flow is negatively regulated by PKCζ activity.